

Review

A Review of Spectral Indices for Mangrove Remote Sensing

Thuong V. Tran ^{1,2,*}, Ruth Reef ¹  and Xuan Zhu ¹ ¹ School of Earth, Atmosphere and Environment, Monash University, Clayton, VIC 3800, Australia² Institute of Engineering and Technology, Thu Dau Mot University, Thu Dau Mot City 75000, Vietnam* Correspondence: thuong.tran@monash.edu

Abstract: Mangrove ecosystems provide critical goods and ecosystem services to coastal communities and contribute to climate change mitigation. Over four decades, remote sensing has proved its usefulness in monitoring mangrove ecosystems on a broad scale, over time, and at a lower cost than field observation. The increasing use of spectral indices has led to an expansion of the geographical context of mangrove studies from local-scale studies to intercontinental and global analyses over the past 20 years. In remote sensing, numerous spectral indices derived from multiple spectral bands of remotely sensed data have been developed and used for multiple studies on mangroves. In this paper, we review the range of spectral indices produced and utilised in mangrove remote sensing between 1996 and 2021. Our findings reveal that spectral indices have been used for a variety of mangrove aspects but excluded identification of mangrove species. The included aspects are mangrove extent, distribution, mangrove above ground parameters (e.g., carbon density, biomass, canopy height, and estimations of LAI), and changes to the aforementioned aspects over time. Normalised Difference Vegetation Index (NDVI) was found to be the most widely applied index in mangroves, used in 82% of the studies reviewed, followed by the Enhanced Vegetation Index (EVI) used in 28% of the studies. Development and application of potential indices for mangrove cover characterisation has increased (currently 6 indices are published), but NDVI remains the most popular index for mangrove remote sensing. Ultimately, we identify the limitations and gaps of current studies and suggest some future directions under the topic of spectral index application in connection to time series imagery and the fusion of optical sensors for mangrove studies in the digital era.

**Citation:** Tran, T.V.; Reef, R.; Zhu, X.A Review of Spectral Indices for Mangrove Remote Sensing. *Remote Sens.* **2022**, *14*, 4868. <https://doi.org/10.3390/rs14194868>

Academic Editor: Chandra Giri

Received: 12 August 2022

Accepted: 26 September 2022

Published: 29 September 2022

Publisher's Note: MDPI stays neutral with regard to jurisdictional claims in published maps and institutional affiliations.



Copyright: © 2022 by the authors. Licensee MDPI, Basel, Switzerland. This article is an open access article distributed under the terms and conditions of the Creative Commons Attribution (CC BY) license (<https://creativecommons.org/licenses/by/4.0/>).

Keywords: vegetation index; mangrove index; mangrove forest; mangrove above ground; biomass; carbon sink; bibliometric analysis

1. Introduction

Mangrove is a term which corresponds to intertidal ecosystems or lignified plant communities that grow in coastal environments between 40°S and 30°N throughout the world (Figure 1). The mangrove boundary is extended to the south of Japan (30.4°N) and Bermuda (32.4°N); to the south of New Zealand (38.05°S), Australia (38.85°S), and the east coast of South Africa (32.98°S) [1,2]. Mangrove distribution is restricted generally to areas where the mean temperature ranges 20–35°C, annual rainfall is between 1500–2500 mm, and there is a substantial riverine input of freshwater discharge [2]. Actually, the number of frozen days in the year may play on mangrove presence at high latitudes [3]. Decreases in the frequency of extreme cold occurrences could lead to considerable increases in mangrove cover near the current poleward limits of mangrove forests. The global mangrove distribution is classified into two groups, including the Indo-West Pacific (IWP) and the Atlantic East Pacific (AEP). Mangroves initially developed on the Tethys Sea's coastlines in the late Cretaceous-early Tertiary period [1,2,4]. Three million years ago, modern mangrove taxa emerged on the eastern borders of Tethys, diversified into present-day IWP regions, and subsequently spread into AEP regions [5,6]. The richness in the distribution of mangrove species reduces from the IWP to AEP. Globally, there are approximately 77 mangrove species, but about 54 species in 20 genera from 16 families constitute the group of “true

mangroves” occurring only in mangrove habitats. Among these 77 species, 65 species in 32 genera and 24 families are recorded from IWP, while only 15 species in 10 genera and 8 families are in AEP [1,2]. The most commonly found genera in both IWP and AEP are *Rhizophora* and *Avicennia* [2].

The biophysical variables of mangroves (i.e., leaf area, basal area, tree height, percent canopy closure, diameter at breast height, carbon stock, and biomass) mostly depend on climatic conditions, while sea level rise has an influence on the structure and spatial distribution of mangroves [7,8]. Temperature, precipitation, and storminess explain 74% of the global trends in the maximum values of canopy height and above-ground biomass [7]. Globally, 75% of mangroves are distributed in tropical regions. The largest cover and highest mangrove diversity are found in Asia (39%), followed by Africa (21%, but mostly on the eastern side), North and Central America (15%), South America (12.6%) and Oceania (Australia, Papua New Guinea, New Zealand, south Pacific islands) (12.4%) [9,10]. The mangroves in the equatorial regions have the maximum biomass and tree canopies can reach an average height of 30–40 m. The highest mangrove forests are found in Gabon, an equatorial African nation, where heights reach 62.8 m. A quarter of the estimated 11.7 Pg C global mangrove carbon stock, which includes soil, above- and below-ground biomass, is stored in Indonesia [7,8]. These biophysical parameters gradually decrease with increasing latitude due to varied temperature and environmental conditions.

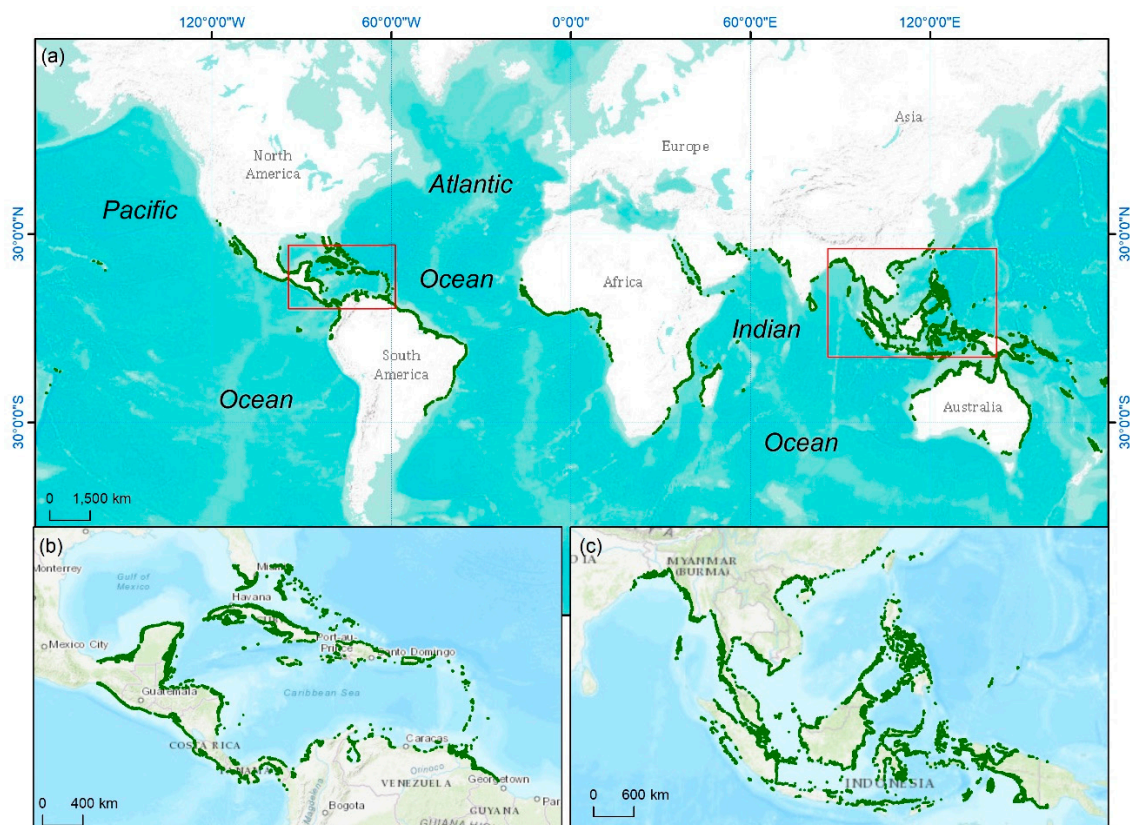


Figure 1. (a) The distribution of mangroves (in pale green) in the world, (b) in the Caribbean, and (c) in South and Southeast Asia (Source: adapted from Global Mangrove Watch, [11,12]).

Mangrove ecosystems produce valuable goods and services, including regulation (e.g., coastal protection, water filtration), supply (e.g., fisheries, aquaculture, timber, fuel, honey, construction materials, medicine), culture (e.g., tourism), and support (e.g., nursery habitats, climate mitigation) [13,14]. In some areas, mangroves have been proposed to provide a natural barrier to coastal erosion process, defending inland areas home to 120 million people from natural hazards (e.g., typhoon, cyclones, tsunamis) [7,15]. Mangrove

restoration for coastal defence is expected to be up to five times more cost-effective than “grey infrastructure” such as breakwaters [16]. Mangroves also regulate water quality, and it is estimated that 2–5 ha of mangroves can treat the effluent from 1 ha of some aquaculture practices [17]. The carbon storage potential of mangroves is 3–5 times higher than that of tropical upland forests due to strong carbon storage in the soil [18,19]. Mangroves are also a valued source of timber, fuel, and tourism. There are over 2000 mangrove related attractions globally, such as boat tours, boardwalks, kayaking, and fishing [20]. Together, the economic value from mangrove ecosystem services has been estimated to exceed 800 billion per year [15,21]. However, approximately 35% of the global mangrove forests has been lost over the past 50 years due to both anthropogenic activities and physical stressors [22,23]. While restoration of mangrove forests has been increasing over the past 40 years, the net reduction in mangrove cover area and species richness is still a high 1–2% per year [22,24].

Traditionally, monitoring mangrove ecosystems used field observation and survey methods [25–27]. However, these approaches are difficult to monitor and measure mangroves in situ due to their dense understory and geographical location in intertidal zones [21,25]. Additionally, field observation and survey methods are labour-intensive, costly, and frequently limited in extent. Many surveys are qualitative and difficult to reproduce or revisit over time. Remote sensing (RS) has overcome the drawbacks of traditional field surveys and is continuously improving in terms of spatial resolution, revisit time and user costs over the past four decades [25,28]. RS is acknowledged in this context as the science and technology of acquisition of information about Earth’s surface materials from a distance, typically from aircrafts or satellites [29]. The two types of remote sensing we refer to are (i) optical and (ii) radar sensors, which are classified according to the energy source of the signal used to identify the object. The remotely sensed data, acquired from these sensors, allows us to gather accurate information about the geographical distribution of mangrove ecosystems and biophysical properties at the pixel level [13,27].

In remote sensing, mangroves can be identified based on the textural and spectral properties of the canopy and leaves [13,30]. Their structural appearance, which can be either homogenous across the forest or heterogeneous, is affected by factors including species composition, growth form, density, and stand height. Almost all mangrove species can be discriminated within the visible and near infrared (NIR) region because of scattering in the spongy mesophyll cells in plants [31,32]. Using structural information extracted from several remotely sensed products regional and global estimation can be made of mangrove height, canopy, species succession, biomass, and carbon stocks [26]. The highest spectral reflectance of mangroves was observed in the NIR region for both Landsat 8 and Sentinel-2A surface reflectance sources (Figure 2). With the Sentinel-2A in particular, mangrove reflectance was observed to rise rapidly at the red-edge. Therefore, mangrove ecosystems can be observed using indices computed from spectral bands in the visible and NIR regions of optical remote sensing.

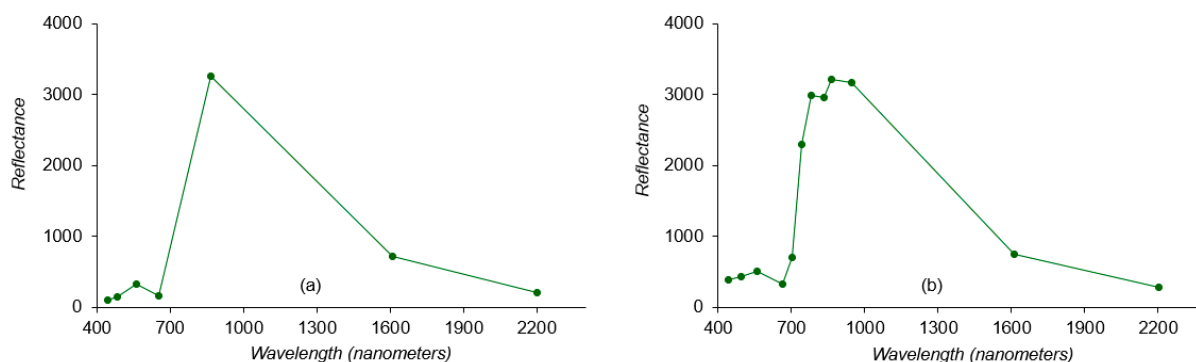


Figure 2. Spectral signatures of mangroves (*Rhizophora*) in Can Gio Mangrove Biosphere Reserve, Vietnam, derived from median values of (a) Landsat 8 and (b) Sentinel-2A surface reflectance in February 2021 (Source: obtained from Google Earth Engine).

The importance of remote sensing in mangrove studies has been recognised in many review studies [25,26,28,30,33–35]. These publications serve as a good starting point for researchers who are interested in mangrove remote sensing. However, the application of different spectral indices in mangroves has not been reviewed extensively in most of these studies. For instance, Green et al. (1998) [33] considered the significance of remote sensing for mangrove mapping from 1972 to 1996. While the study is the first paper that mentioned applying NDVI to mangrove classification, it only focused on NDVI even though at the time there were over 40 vegetation indices that could have been relevant to mangrove ecosystems. During the 1998–2018 period, most review papers highlighted remote sensing as a technique or approach for mangrove studies, while remote sensing has been defined as the science of acquiring information from distance [29,36,37]. Recently, Wang et al. (2019) [25] revealed common gaps in previous publications (i.e., research topics, key milestones, and mangrove driving forces) in mangrove remote sensing and investigated the importance of remote sensing for mangrove studies from 1956 to 2018. However, Wang et al. (2019) did not clearly state what kinds of spectral indices are specifically applied to mangrove remote sensing.

The present study intends to address the aforementioned knowledge gaps, by answering the following research question: what spectral indices have been applied and have been proven effective for mangrove remote sensing? Our objectives are to (i) examine and categorise spectral indices used in publications related to mangrove remote sensing; (ii) assess their applications in the study of mangrove ecosystems; and (iii) propose future directions for the application of additional spectral indices in mangrove remote sensing.

2. Search Strategy and Data Analysis

Mangrove scholars used various qualitative and quantitative approaches to understand and organise earlier findings of mangrove studies. Among these, a quantitative analysis of academic literature, defined as bibliometrics, was investigated as a potential tool to introduce a systematic, transparent, and reproducible review process [38–41]. Compared to other literature review techniques, bibliometric analysis of the published literature is effective to identify research gaps and direct future avenues of research [41]. For bibliographic citations, Web of Science (WoS) and the Scopus platforms are the most extensive databases which are widely used to obtain metadata for bibliometric analysis [42,43]. Scopus was launched in 2004, but WoS launched in 1997 and is considered the earliest international bibliographic database [42,44]. WoS comprises four citation databases with more than 10,000 journals [45]. Journals indexed in the WoS must meet 28 criteria (i.e., 24 quality criteria and 4 impact criteria) [44,46]. The fulfilment of 28 criteria contributes to enhancing academic quality and minimising the influence of multiple predatory journals. The journal listed in the WoS database primarily provides impact factor (a ratio between citations and citable items published the previous year) and h-index (an index based on a list of publications ranked in descending order by Times Cited count) [46]. Therefore, journals with high impact factor or h-index are cited more often than journals with lower impact factor or h-index.

Various keywords were entered in the searching process associated with global mangrove ecosystems based on spectral indices application (Table 1). We used Thomson Data Analyzer (TDA) integrated in the Web of Science (WoS) Core Collection to retrieve annual publications and their citations [47]. The keyword search resulted in 293 papers published between 1992 and 2021. We then reviewed the abstract and content of the 293 papers and removed from our study the papers that did not relate to the application of spectral indices in mangroves. This left 195 publications (including 90 journal papers, 14 conference papers and one book chapter) for our review.

Table 1. The predefined keywords of the searching process.

No.	Keywords
1	vegetation index and mangrove
2	comprehensive mangrove quality index
3	a mangrove recognition index
4	mangrove and an index analysis approach
5	leaf area index and mangrove
6	spectral mangrove index

Full records (i.e., author, title, source, abstract) and cited references of the search results were downloaded in the BibTex format in several batches, each comprising no more than 500 data entries. For further processing, all of the obtained result files were zipped together and imported into the R-statistical and VOSviewer software packages. The bibliometric analysis was carried out with the help of Bibliometrix package in R [38]. The annual cited times of the gathered articles were calculated using TDA's citation report tool, while the top journal sources for publication and citation were determined using Bibliometrix package. Finally, using VOSViewer software [48], we performed co-word analysis to visualise density networks of author keywords for trend analysis in mangrove remote sensing. The co-word method is a technique to analyse the co-occurrences of key words and identify relationships and interactions between the topics researched and emerging research trends [48]. Details regarding the theory and practical function of the co-word approach utilising VOSViewer software may be found at [45,48]. However, the record of the online bibliographic database prior to 1990 may be incomplete [42,44,49] because the internet-based Web of Science was firstly launched in 1997. Therefore, several publications from print only sources may be missing. We thus supplemented our database with metadata from outcomes of Green et al. (1998) [33] and Bannari et al. (1995) [50] to increase the number of studies applying spectral indices in mangrove studies prior to 1996.

Publications and annual citations in this field of research, retrieved from citation report analytics of the Web of Science Core Collection, significantly increased between 1996 and 2021 (Figure 3). The number of publications dropped in 2021, which may be related to COVID-19 pandemic because most field trips were delayed or cancelled and this impacted field data collection for validation and other known impacts on academic workloads [51]. Most of the publications (21) were published in the journal of Remote Sensing (IF: 4.848, Open access), others were mainly from the International Journal of Applied Earth Observation and Geoinformation (8, IF: 5.993, Open access), International Journal of Remote Sensing (8, IF: 3.362), Estuarine, Coastal and Shelf Science (7, IF: 2.904), Modeling Earth Systems and Environment (6, IF: N/A) and ISPRS Journal of Photogrammetry and Remote Sensing (5, IF: 10.565). The journals Ecological Indicators, Regional Studies in Marine Science, and Wetlands had four papers each. The remaining journals had published less than three papers involving mangrove remote sensing since 1996. In-text citations of work that applied mangrove remote sensing indices were found in Remote Sensing of Environment (881, h-index: 281), Remote sensing (445, h-index: 124), International Journal of Remote Sensing (437, h-index: 174), Estuarine, Coastal and Shelf Science (249, h-index: 134), Aquatic Botany (170, h-index: 94). The publications most cited were those in higher ranked (higher IF) journals, regardless of the open access status of the journal.

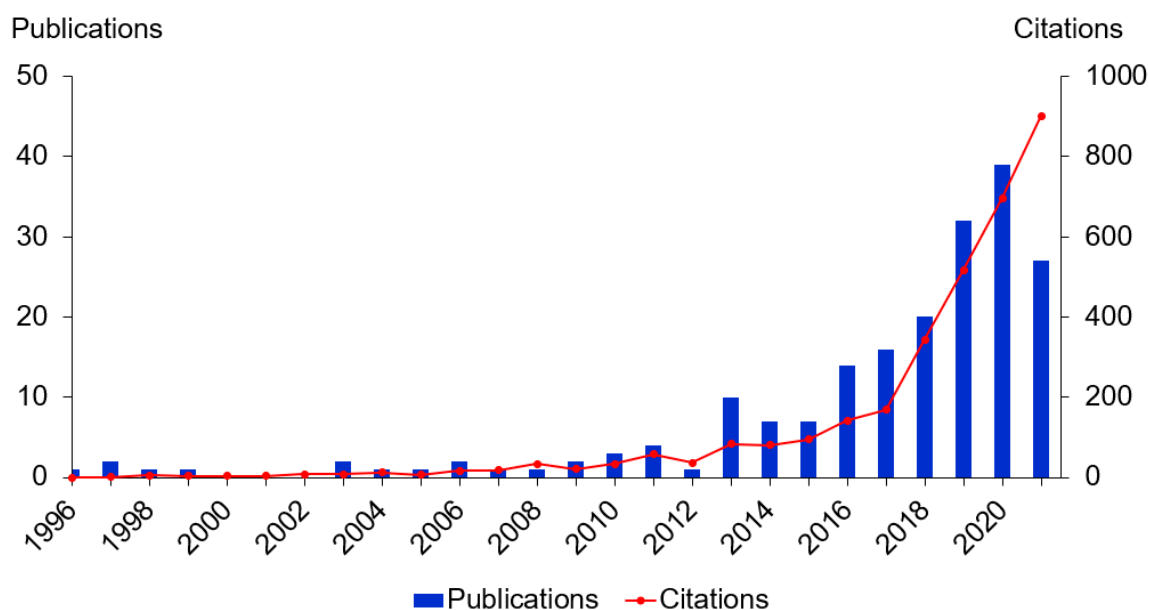


Figure 3. Change in 195 peer-reviewed publications and their citations per year between 1996 and 2021 (based on the citation report tool in TDA using mentioned keywords).

3. Overview of Spectral Indices Used in Mangrove Remote Sensing

A spectral index is an equation that combines pixel values from two or more spectral bands in a multispectral image using various algorithms, mainly focused on band ratio or feature scaling (e.g., normalised or standardised algorithms) [52,53]. Spectral indices are calculated to highlight pixels in an image that not only show the relative abundance of a land cover of interest, but also emphasise an ecosystem function [52–54]. They show better sensitivity than individual spectral bands for spectral signature detection. Throughout the mission of Earth surface observation, spectral indices have significantly contributed a more thorough understanding of environments and ecosystems across space and time [28]. The geographical extent of mangrove studies using spectral indices has also seen a significant change over time (Table 2). Most studies (92%) were carried out at the national level, while a few publications implemented research on intercontinental/global scale during the 2000–2015 period and this trend is increasing (16% in 2021 vs. 8% in 2016). The study areas were mainly in India (12.8%), Mainland China (12.3%), Indonesia (9.7%), the US (9.7%), and Mexico (8.2%).

Table 2. The mangrove study area of spectral indices application, obtained from our searched publications.

Country/Region	Before 2000s	2001–2015	2016–2021	%
US	2 (33%)	6 (15%)	11 (7%)	9.7
Mexico	1 (17%)	6 (15%)	9 (6%)	8.2
India	0	6 (15%)	19 (13%)	12.8
China	0	3 (8%)	21 (14%)	12.3
Australia	0	1 (3%)	6 (4%)	3.5
Malaysia	0	5 (13%)	7 (5%)	6.2
Indonesia	0	1 (3%)	18 (12%)	9.7
Vietnam	0	1 (3%)	7 (5%)	4.1
Others	3 (50%)	7 (18%)	29 (19%)	20
Intercontinental regions and globe	0	3 (8%)	25 (16%)	13.5

Spectral indices can be categorised as either satellite or airborne system indices based on the platforms used for data acquisition. Depending on the spectral bands of passive satellite remote sensing, spectral indices may be further grouped into indices with (i)

simple ratio, (ii) visible and near-infrared (VNIR) bands, (iii) visible and red edge bands, (iv) visible and mid-infrared bands, and (v) visible and shortwave infrared (SWIR) bands. In addition, following the applications of spectral indices in mangrove remote sensing, we separate spectral vegetation indices and spectral mangrove-specific indices. The key differences between the two types of indices are their applications and the spectral bands used in the indices. Vegetation indices are spectral indices computed using spectral bands in the visible, red edge, and near-infrared regions [55]. They have been widely applied to mangrove ecosystems previously [13,30]. However, as mangroves have common spectral characteristics as other vegetation, separating mangroves from other types of vegetation using a single vegetation index is challenging [56]. To address this issue, some mangrove-specific spectral indices have been proposed for separating mangroves from terrestrial vegetation [56–60]. These spectral mangrove indices include spectral bands from VNIR to SWIR regions. In this review, based on publications that used spectral indices for mangrove ecosystems and the approaches they applied, we classified indices into four categories: (i) visible and near-infrared bands; (ii) visible and red edge bands; (iii) visible bands of airborne systems; and (iv) spectral mangrove specific- indices.

3.1. Spectral Indices with Visible and Near-Infrared Bands (VNIR)

Indices measured from spectral bands in the VNIR regions are acknowledged as vegetation indices [50], except Normalized Difference Water Index (NDWI) [61]. The history of spectral vegetation indices development is associated with the Landsat mission in 1972. Particularly, Pearson and Miller (1972) developed the first vegetation indices, i.e., Ratio Vegetation Index (RVI) and Vegetation Index Number (VIN), to estimate and monitor vegetative cover [50,62]. Following Pearson and Miller (1972), Rouse et al. (1973) introduced the Normalized Difference Vegetation Index (NDVI) that is now widely applied for land cover and environmental studies [63,64]. Over the last four decades, more than 40 vegetation indices have been developed, but 28 of these were used in mangrove investigations (Table 3). Two categories of vegetation indices can be separated: ones that include only spectral bands and others that include spectral bands that are adjusted by non-spectral factors [e.g., soil adjustment factor (L), soil line factors (a , b), and coefficients of atmosphere resistance (c_1 and c_2)]. The first category (e.g., RVI, VIN, NDVI—Table 3) is based on linear combinations (difference or sum) of spectral bands or raw band ratios without considering environmental interactions. The second group (e.g., SAVI, TSAVI, EVI—Table 3) is based on the knowledge of physical phenomena which explains interactions between electromagnetic radiation, the atmosphere, the vegetative cover, and the soil background.

In the first group without adjustment factors, NDVI is the first index to show the highest correlation with field measured mangrove canopy cover ($r = 0.91$), higher than PVI, GVI, and RVI [65]. NDVI (No.3—Table 3) is a simple indicator that is acquired in red (visible) and near-infrared (NIR) regions, based on a normalised algorithm. The NIR band in the NDVI equation is useful for vegetation detection because healthy vegetation (which contains chlorophyll) reflects more NIR compared to other wavelengths [63]. The normalised algorithm mitigates the atmospheric effects and the impacts of sensor calibration degradation in the red and NIR bands [64,66]. Mathematically, NDVI also forms the basis for other indices. For example, a bijective relationship between NDVI and VIN is demonstrated by Equation (1). However, the NDVI values are affected by soil background when the green leaf area is small or the majority of the scene is soil [67,68]. Therefore, a number of vegetation indices in the second category have been developed for taking into account environmental conditions. For example, to adjust soil background, soil factors (e.g., L , a , and b) were included in SAVI and TSAVI (No.8–9, Table 3). Both indices SAVI and TSAVI are equal to NDVI, if the value of the soil adjustment factor in SAVI (No. 8, Table 3) is zero ($L = 0$) or the slope (a) and ordinate (b) at the origin of bare soil line parameters in TSAVI (No.9, Table 3) are one and zero ($a = 1$ and $b = 0$), respectively.

$$NDVI = \frac{NIR - R}{NIR + R} = \frac{NIR/R - 1}{NIR/R + 1} = \frac{VIN - 1}{VIN + 1} \quad (1)$$

Some studies show that the indices that include adjustment factors are less sensitive to atmospheric and soil background effects than the first-generation spectral indices [50,64,65]. Enhanced Vegetation Index (EVI, No.4–Table 3) [69], for example, which corrects for some atmospheric conditions and canopy background noise, and provides a better estimation of mangrove biophysical properties in high density forests than does NDVI [70]. However, the blue band requirement may be a disadvantage of EVI, which cannot be generated from optical sensors that do not have a blue band, such as the Advanced Very High-Resolution Radiometer (AVHRR) and the Advanced Spaceborne Thermal Emission and Reflection Radiometer (ASTER). Alternatively, the EVI-2 (No.28–Table 3) with two spectral bands in the red and NIR regions was proposed, achieving similar performance to EVI, which can be produced by almost all optical sensors [71]. However, the EVI-2 is sensitive to the impact of the bidirectional reflectance distribution function (BRDF). Therefore, each index has advantages and disadvantages in relation to vegetation characteristics with overlapping spectral features due to background signals from soil and confounding factors (e.g., sensor and calibration effects, quality assurance and quality control, BRDF, and atmospheric and topographic effects). Hence, there are no perfect vegetation indices for all aspects of mangrove studies under all conditions.

Table 3. The 28 indices in the spectral wavelength 400–1000 nm used in mangrove research (R: Red; G: Green; B: Blue; and NIR: Near Infrared). For whole algorithms, L is a soil adjustment factor that addresses nonlinear model, differential NIR and red radiant transfer through a canopy [72]; a and b are soil line factors [73]; c_1 and c_2 are coefficients of atmosphere resistance term which use blue band to correct for aerosol influences in red band [69].

No.	Spectral Index	Formula	Reference
1	Vegetation Index Number [62]	$VIN = \frac{R}{NIR}$	[74,75]
2	Ratio Vegetation Index [62]	$RVI = \frac{NIR}{R}$	[58,59,65,76–91]
3	Normalized Difference Vegetation Index [63]	$NDVI = \frac{NIR-R}{NIR+R}$	From 1991 to 2011: [65,76–78,92–105] Since 2012: [58–60,74,75,80–87,89–91,106–209] [3,59,74,75,80,82,84,90,123,144,146,149,153,160,169,172,176,186,191,196,197,201,206,207,210–225]
4	Enhanced Vegetation Index [69]	$EVI = \frac{2.5(NIR-R)}{NIR+c_1R-c_2B+L}$	[76,138]
5	Perpendicular Vegetation Index [73]	$PVI = \frac{NIR-aR-b}{\sqrt{a^2+1}}$	[227]
6	Normalized Green-red Difference Index [226]	$NGRDI = \frac{G-R}{G+R} + 0.08$	[74–76,84,97]
7	Difference Vegetation Index [228]	$DVI = NIR - R$	[58,76,83–85,89–91,108,110,120,123,132,138,139,145,146,150,169,170,201,207,225]
8	Soil Adjusted Vegetation Index [67]	$SAVI = (1+L) \frac{NIR-R}{NIR+R+L}$	[76,196]
9	Transformed soil adjusted vegetation index [68]	$TSAVI = \frac{a(NIR-aR-b)}{R+aNIR-ab}$	[76]
10	Soil adjusted ratio vegetation index 2 [229]	$SAVI_2 = \frac{NIR}{R+a+b}$	[74,75,84,109,139,196]
11	Global environment monitoring index [230]	$GEMI = n(1 - 0.25n) - \frac{R-0.125}{1-R}$ at $n = \frac{2(NIR^2-R^2)+1.5NIR+0.5R}{NIR+R+0.5}$	[74,84,196,232]
12	Atmospherically Resistant Vegetation Index [231]	$ARVI = \frac{NIR-2R+B}{NIR+2R-B}$	[83]
13	Non-linear vegetation index [233]	$NLI = \frac{NIR^2-R}{NIR^2+R}$	[81,85,86,108,132,145,169,191,207]
14	Modified soil-adjusted vegetation index [234]	$MSAVI = \frac{2NIR+1-\sqrt{(2NIR+1)^2-8(NIR-R)}}{2}$	[81,85,108]
15	Renormalized difference vegetation index [235]	$RDVI = \frac{NIR-R}{\sqrt{NIR+R}}$	[85,145]
16	Modified Simple Ratio [236]	$MSR = \frac{NIR/R-1}{\sqrt{NIR/R+1}}$	[130,196]
17	Green Normalized Difference Vegetation Index [237]	$GARI = \frac{NIR-[G-1.7*(B-R)]}{NIR+[G-1.7*(B-R)]}$	

Table 3. Cont.

No.	Spectral Index	Formula	Reference
18	Optimized Soil Adjusted Vegetation Index [238]	$OSAVI = \frac{NIR-R}{NIR+R+0.16}$	[82,89,109,110,115,130,177,199]
19	Green Normalized Difference Vegetation Index [239]	$GNDVI = \frac{NIR-G}{NIR+G}$	[81,85,87,89,119,139,145,193,207]
20	Green Leaf Index [240]	$GLI = \frac{(G-R)+(G-B)}{(G+R)+(G+B)} + 0.07$	[227]
21	Triangular Vegetation Index [241]	$TVI = 0.5 \times [120(NIR - G) - 200(R - G)]$	[74,82,84,85,108,207]
22	Transformed Difference Vegetation Index [242]	$TDVI = 1.5 \left[\frac{NIR-R}{\sqrt{NIR^2+R+0.5}} \right]$	[109,115]
23	Modified Non-Linear Vegetation Index [243]	$MNLI = \frac{1.5(NIR^2-R)}{NIR^2+R+0.5}$	[83]
24	Modified Chlorophyll Absorption Ratio Index 1 [244]	$MCARI_1 = 1.2 \times [2.5(NIR - R) - 1.3(NIR - G)]$	[85,89,199,232]
25	Modified Chlorophyll Absorption Ratio Index 2 [244]	$MCARI_2 = \frac{MTVI_2}{1.5[1.2(NIR-G)-2.5(R-G)]}$	
26	Modified Triangular Vegetation Index [244]	$\frac{\sqrt{(2NIR+1)^2 - (6NIR-5\sqrt{R})} - 0.5}{G^2}$	
27	Chlorophyll Vegetation Index [245]	$CVI = \frac{NIR \cdot R}{G^2}$	[119,145,196]
28	Enhanced Vegetation Index 2 [71]	$EVI_2 = 2.5 \left(\frac{NIR-R}{NIR+2.4R+L} \right)$	[59,74,75,84,89,132,193,196,207,246]

3.2. Spectral Indices in Visible and Red-Edge Bands

The red edge is a band in the red-NIR transition zone that indicates the transition between red visible absorption by chlorophyll and NIR scattering due to leaf internal structure [25]. This transition zone is used in various vegetation indices, the most important of which is the normalised difference between red visible (0.6 nm) and NIR (0.8 nm) reflectance. Spectral indices obtained from the red edge region (Table 4) were used in several investigations for mangrove chlorophyll and biophysical parameters [81,119], mangrove density and carbon analyses [85,247], and mangrove biomass [207]. These investigations found strong correlation ($r > 0.95$) between ground truth data and red edge vegetation indices. Normally, red edge bands are available from hyperspectral datasets that are difficult for large-scale collection. Alternatively, since 2015, three red-edge bands have been incorporated in the Sentinel-2A sensor, which could be combined with other visible bands to provide essential information about mangrove ecosystems at a spatial resolution of 10 m. Therefore, the use of red-edge bands promises the potential to benefit mangrove ecosystems associated with mangrove health monitoring in the future.

Table 4. The used indices with VNIR and red-edge bands (R: Red; B: Blue; and NIR: Near Infrared). With three Red-edge bands of Sentinel-2A, each formula can compute three sub-equations.

No.	Spectral Index	Formula	Reference
1	Normalised Difference Index [248]	$NDI = \frac{R_{edge}-R}{R_{edge}+R}$	
2	Red edge NDVI [249]	$NDVI_{Red-edge} = \frac{NIR-R_{edge}}{NIR+R_{edge}}$	[81,85,119,207,247]
3	Plant Senescence Reflectance Index [250]	$PSRI = \frac{R-B}{R_{edge}}$	
4	Normalized Difference Red edge Index [251]	$NDRE = \frac{NIR-R_{edge}}{NIR+R_{edge}}$	
5	Red-edge Chlorophyll Index [252]	$CI_{Red-edge} = \frac{NIR}{R_{edge}} - 1$	
6	MERIS Terrestrial Chlorophyll Index [253]	$MTCI = \frac{NIR-R_{edge}}{R_{edge}-R}$	

3.3. Spectral Indices with Visible Bands of Airborne Systems

Traditionally, aerial photographs (AP) were widely used for mangrove mapping and assessment [94]. Nowadays, with the support of Unmanned Aerial Vehicles (UAVs) or drones, the application of aerial photographs has become more convenient. Some spectral indices for mangrove classification have been proposed using visible bands of aerial photographs that can achieve an overall accuracy of over 95% in mangrove cover mapping [157,254] (Table 5). Notably, integration of Red-edge, NIR, and shortwave infrared (SWIR) bands in the optical sensors of UAVs promises an advantage for monitoring mangrove ecosystems at a spatial resolution of centimetres. This drone-based multispectral remote sensing can be as the future for mangrove remote sensing. However, these applications are only suitable for a small area and can be employed in a short time due to cost and energy limitation. More importantly, the use of UAVs for field data collection is regulated by the government in most countries throughout the world.

Table 5. The used UAV spectral indices for mangrove ecosystems.

No.	Spectral Index	Formula	Reference
1	Excess Green Vegetation Index [248]	$ExG = 2 \times G - R - B + 50$	
2	Normalized Difference Index [248]	$NDI = \frac{G-R}{G+R}$	
3	Negative Excess Red Vegetation Index [255]	$NegExR = G - 1.4 \times R$	[196,227,254]
4	Visible Atmospheric Resistant Index [256]	$VARI = \frac{G-R}{G+R-B}$	
5	Colour Index of Vegetation Extraction [257]	$CIVE = 0.441R - 0.881G + 0.385B + 18.78745$	
6	Vegetative Index [258]	$VEG = \frac{G}{R^{0.667}} \times B^{0.333}$	
7	Excess Green minus Excess Red [259]	$ExG - ExR$	
8	Triangular Greenness Index [260]	$TGI = G - 0.39R - 0.61B$	
9	Combined Index [261]	$CI = 0.25ExG + 0.3ExGR + 0.33CIVE + 0.12VEG$	
10	Visible-band Difference Vegetation Index [262]	$VDVI = \frac{2G-B-R}{2G+B+R}$	

3.4. Mangrove-Specific Spectral Indices

Mangroves are found in coastal wetlands where they are regularly submerged by tides [55,60,263]. As a result, fluctuations in tide levels, and thus the presence of water, results in tide-dependent variation in spectral signatures for mangrove forests, leading to inaccurate mapping results, particularly in locations with large tidal ranges [57,135]. Recently, several studies have developed specific spectral indices that can adapt to changes in tide conditions and applied them in order to separate mangroves from non-mangroves [57,58,60] and from other land cover types [55]. These are the mangrove-specific indices. During the 2013–2021 period, six mangrove-specific indices were proposed to improve the accuracy of single image remotely sensed data during high tide (Table 6).

Zhang and Tian (2013) [57] proposed a mangrove recognition index (MRI–Equation (2)) for mangrove detection using multi-temporal Landsat TM images that is insensitive to the stage of the tide. Winarso et al. (2014) [56] further developed this method to create a mangrove discrimination index (MDI–Equation (3)) for estimate mangrove density from Landsat 8 images. Kumar et al. (2017) [59] proposed two new vegetation indices (Normalised Difference Wetland Vegetation Index and Shortwave Infrared Absorption Index) and combined them with two previously published indices (Normalised Difference Infrared Index and Atmospherically Corrected Vegetation Index) to integrate the Mangrove Probability Vegetation Index (MPVI–Equation (4)) for mangrove classification. Gupta et al. (2018) [58] published a Combined Mangrove Recognition Index (CMRI–Equation (5)) to distinguish mangrove from non-mangrove with an accuracy of more than 60%. Jia et al. (2019) [60] generated the Mangrove Forest Index (MFI–Equation (6)) using spectral bands from Sentinel-2 data to detect submerged mangrove forests at high tide.

Table 6. The proposed mangrove indices for mangrove classification (EQN: equation number). In the Equation (2), GVI and WI are green vegetation index and wetness index at low (L) tide and high (H) tide, respectively. In Equation (4), n is the total number of bands in the image, R_i is the reflectance value at band i for a pixel of the reflectance image, and r_i is the reflectance value at band i for candidate spectrum of mangrove forest. In Equation (6), the ρ_{λ} is the reflectance of the band centre of λ , and i ranged from 1 to 4; $\lambda_1, \lambda_2, \lambda_3, \lambda_4$ represent the centre wavelengths at 705, 740, 783 and 865 nm, respectively. λ_i is the baseline reflectance in λ_i . ρ_{665} and ρ_{2190} are the reflectance of band 4 (centred at 665 nm) and 12 (centred at 2190 nm), respectively. In Equations (3), (5), and (7), G , R , NIR , and $SWIR$ are green, red, near-infrared, and shortwave infrared bands, respectively.

Index	Formula	EQN	Reference
Mangrove Recognition Index	$MRI = GVI_L - GVI_H \times GVI_L \times (WI_L + WI_H)$	(2)	[57]
Mangrove Damage Index	$MDI = \frac{NIR-SWIR}{NIR \times SWIR} \times 10,000$	(3)	[56]
Mangrove Probability Vegetation Index	$MPVI = \frac{n \sum_{i=1}^n R_i r_i - \sum_{i=1}^n R_i \sum_{i=1}^n r_i}{\sqrt{n \sum_{i=1}^n R_i^2 - \left(\sum_{i=1}^n R_i\right)^2} \sqrt{n \sum_{i=1}^n r_i^2 - \left(\sum_{i=1}^n r_i\right)^2}}$	(4)	[59]
Combined Mangrove Recognition Index	$CMRI = \frac{NIR-R}{NIR+R} - \frac{G-NIR}{G+NIR}$	(5)	[58]
Mangrove Forest Index	$MFI = [(\rho_{\lambda 1} - \rho_{B\lambda 1}) + (\rho_{\lambda 2} - \rho_{B\lambda 2}) + (\rho_{\lambda 3} - \rho_{B\lambda 3}) + (\rho_{\lambda 4} - \rho_{B\lambda 4})]/4$ $\rho_{B\lambda i} = \rho_{2190} + (\rho_{665} - \rho_{2190}) \times (2190 - \lambda_i) / (2190 - 665)$	(6)	[60]
Mangrove Vegetation Index	$MVI = \frac{NIR-G}{SWIR_1-G}$	(7)	[55]

These proposed mangrove indices involve the signature of mangroves in the context of tidal fluctuation, which is sensitive to greenness and wetness patterns. Thus, MRI and MPVI are sensitive to tidal extent and period, and cannot be used in site comparisons where sites differ in hydrology. Additionally, the number of spectral bands required for the MFI calculation is only available using Sentinel-2 or hyperspectral sensors. Baloloy et al. (2020) [55] recently analysed the shortcomings of earlier integrated mangrove forest indices (i.e., MRI, CMRI, MPVI, NDI, and MFI) and developed a new index: the mangrove vegetation index (MVI—Equation (7)), for enhancing the accuracy of mangrove forest extent mapping. MVI is a single index that classifies mangroves, terrestrial vegetation (forest and non-forest), bare soil, built-up areas, water, and clouds using reflectance data from Sentinel-2A and Landsat-8 in the NIR, Green, and SWIR bands. MVI validation was initially used at an intercontinental scale and demonstrated an accuracy of more than 80% for the entire set of geographical research locations. The high index accuracy of MVI can provide a possibility for global mangrove studies, although MVI is limited by biophysical and environmental parameters due to its reliance on SWIR. Using the SWIR spectrum, in particular, has been a problem for sensor systems constructed with solely visible and NIR wavelengths (e.g., Landsat-1,4 and PlanetScope). Additionally, SWIR reflectance value is frequently mixed with built-up land noise, water bodies, and vegetation surrounding [61,264,265]. Neri et al. (2021) [266] investigated misclassification of mangroves from other land cover types in aquaculture zones, irrigated croplands, and palm tree sites when applying MVI due to spectral similarity between mangroves and vegetation in these areas. Notably, the significant drawback of MVI is that it does not have a specific optimal threshold for mangroves, which differs from ranges of vegetation and other mangrove-specific indices for mangrove separation.

In summary, there are several newly improved spectral indices for mangrove classification, but none of these can completely reduce the impact of environmental factors (e.g., tidal influences, land cover mixture).

4. Evaluation of Spectral Indices Applications in Mangrove Remote Sensing

As mentioned in Section 3, a variety of spectral indices have been used for (i) mapping mangrove extents and distributions; (ii) measuring above-ground properties of mangroves; and (iii) detecting mangrove changes. The co-word map of keywords that resulted from the

co-word analysis of the literature on spectral indices application for mangroves is presented in Figure 4. The mangrove and forest were core words of the network, and NDVI and remote sensing were prominent terms in a field study. This showed that NDVI has a strong relationship with aspects of mangrove remote sensing in terms of spectral index application. Also, the result predicted that NDVI was the most common index applied to mangrove ecosystems. In total, 82% of our reviewed publications used NDVI and 28% used EVI.

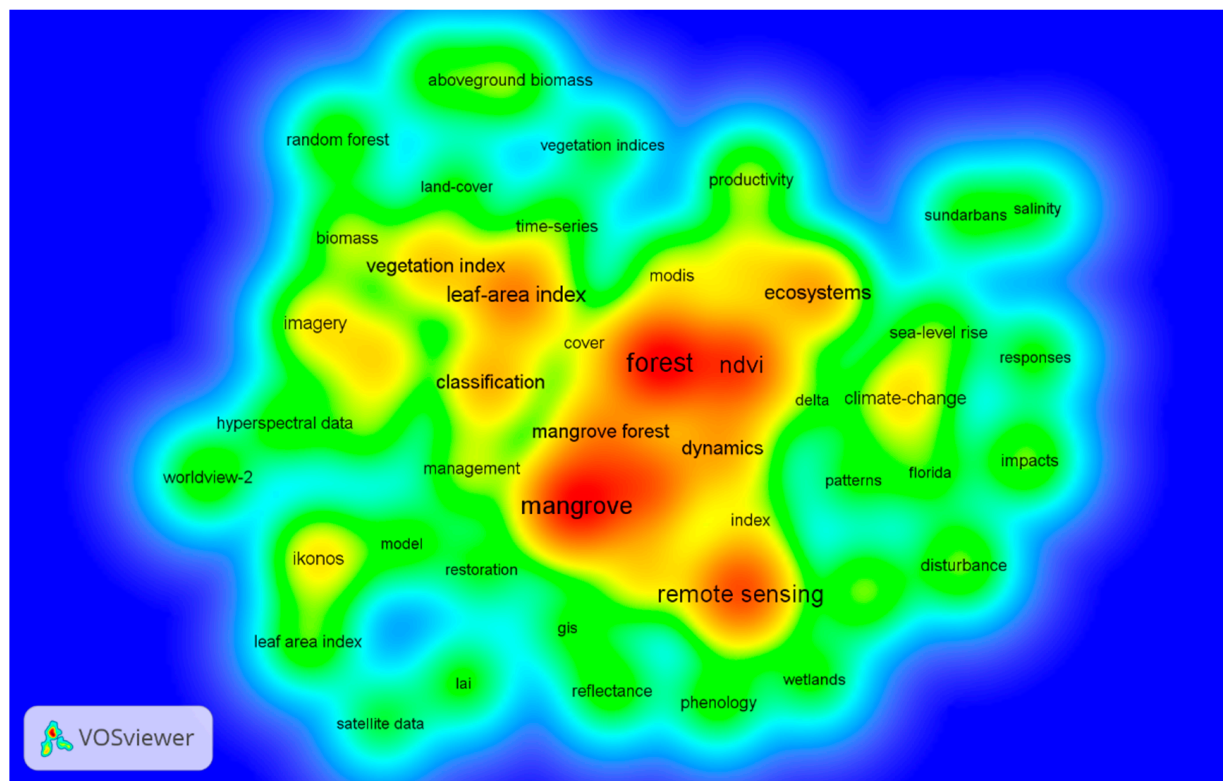


Figure 4. Co-word keywords map of spectral indices' application in mangrove research. Colours indicated the density of keywords or terms, ranging from blue (lowest density) to red (highest density). The larger the number of items in the vicinity of a point and the higher the weights of the neighbouring items, the closer the point is to being red.

4.1. Mangrove Extent and Distribution

Mapping mangroves is important for recording the present mangrove area and species distribution, provides information to support management decisions around potential threats of degradation due to uncontrolled development, and enables modelling change in relation to driving factors. Mangrove mapping can be binary, which classifies an image into two classes: mangroves and non-mangroves, or into a number of land covers based on a particular land cover classification scheme with mangrove as one of the land cover types. Binary mapping normally uses single spectral indices (e.g., NDVI, EVI, SAVI, or mangrove indices) to highlight the pixels of mangrove vegetation and separate them from non-mangrove pixels [58]. Mapping can also include continuous classifiers such as height and canopy area.

Image classification for mangrove mapping can be supervised or unsupervised, pixel-based or object-based. Almost all previous research applied composited bands of satellite images based on classification approaches such as unsupervised algorithms (e.g., ISODATA or K-means) and parametric supervised algorithms (e.g., maximum likelihood) to detect mangrove extents without spectral indices application [25,26,267]. The overall accuracy of post-classification from these approaches ranges from 42% to 68% for most optical sensors and methodologies to measure accuracy [26]. Since spectral indices were used

for mangrove ecosystems under pixel-based or object-based categories based on machine learning algorithms (e.g., artificial neural network, support vector machine, and random forest), an improvement of post-classification overall accuracy has been achieved to more than 80% [26]. More recent studies have used mangrove classification using spectral indices based on random forest, one of the machine learning algorithms, and offer the highest post-classification overall accuracy (>92%) [27,196,268].

From using single spectral indices for mangrove separation, some studies found that in dense mangrove areas, the NDVI or EVI value threshold for discriminating mangroves was 0.3 and above [104,269]. Le et al. (2020) applied NDVI, derived from Sentinel-2, to detect mangrove cover in the Can Gio Mangrove Biosphere Reserve, Vietnam [183]. This study considered that the NDVI mangrove value as $NDVI > 0.3$ with an overall classification accuracy of 83%. In addition to NDVI/EVI, six mangrove spectral indices (Table 6) have been developed and applied for mangrove separation with an overall classification accuracy of 80% above [55].

Vegetation, soil, and water are the three principal factors that contribute to the pixel composition of remotely sensed data in mangroves (Figure 5). In addition, seasonal and diurnal intertidal interactions influence the surface appearance [13,263]. These factors have a significant impact on the spectral characterisation of picture components. Therefore, depending on the effects of natural surroundings and mangrove density, the NDVI/EVI thresholds can be adjusted. In addition to physical influences, mangroves and other types of vegetation may generate similar signals from the vegetation index [56]. As a result, utilising a single NDVI or EVI threshold to distinguish mangroves from other types of vegetation may lead to an inaccurate outcome. Therefore, several soil and water spectral indices (Table 7) have been used concurrent with vegetation indices to improve mangrove detection [150,198].



Figure 5. Mangroves in Victoria State, Australia (Source: photo taken by author).

Table 7. The indices in the Visible, Near Infrared (NIR), and Shortwave Infrared (SWIR) bands.

No.	Spectral Index	Formula	Reference
1	Normalized Difference Moisture Index or Land Surface Water Index [264,270,271]	$NDMI = LSWI = \frac{NIR - SWIR}{NIR + SWIR}$	[59,60,91,123,134,135,152,191,198,201]
2	Normalised Difference Water Index [264]	$NDWI = \frac{R - SWIR}{R + SWIR}$	[97,105,138,150,195,206]
3	Modified Normalized Difference Water Index [272]	$MNDWI = \frac{G - SWIR}{G + SWIR}$	[60,134,201]
4	Normalised Difference Soil Index [105]	$NDSI = \frac{SWIR - NIR}{SWIR + NIR}$	[105]
	Normalized Difference Water Index [61]	$NDWI = \frac{G - NIR}{G + NIR}$	[58,130,195,196,198,201]

The reflected signals from the SWIR regions capture information on radiation absorption by water, cellulose and lignin, and a variety of other biological elements. Nevertheless, collecting satellite imagery at SWIR wavelengths has distinct advantages, such as better atmospheric penetration and better contrasts among different vegetation types. The utilisation of the SWIR band in conjunction with the visible and NIR bands, in particular, aids in enhancing the presence of water in plant leaves [264] or urban characteristics [265]. For example, NDWI and NDBI threshold values more than 0 visualise water bodies and impervious surface, respectively [61,264,265]. Besides, several studies used elevation data and tasselled cap transformation to further improve the classification accuracy [55,57,134]. Consequently, an improved performance ($\geq 90\%$ of overall accuracy) was investigated when apply multiple spectral indices for detecting the mangrove cover [27,267].

Our search did not reveal a spectral index that has been applied for mangrove species separation. Previous studies applied spectral bands to separate mangrove species based on maximum likelihood classification or machine learning algorithms (e.g., random forest and support vector machine) because each mangrove specie reflects a particular wavelength of the spectrum [25–27,164,273]. These studies revealed that spectral reflectance properties of some mangrove species are similar, making a challenge for identification. Hirata et al. (2014) [273] proved that the spectral reflectance properties for *A. alba* and *S. alba* were clearly distinct in three of four VNIR bands (i.e., Green, Red, and NIR), whereas those for the *Rhizophora* and *Bruguiera* species were similar in most spectral bands. A similarity of spectral bands among mangrove species leads to a uniformity/resemblance as using spectral indices because spectral index is computed from spectral bands ratio. It shows that almost all of mangrove species also have the same threshold value in spectral index. For instance, red mangroves (*Rhizophora*), black mangroves (*Avicennia*), and white mangroves (*Laguncularia racemosa*) may have particular spectral reflectance in a single spectral band, but the signals of three species in NDVI/EVI are normally more than 0.3.

4.2. Above-Ground Properties of Mangroves Estimation

The term “above-ground mangroves properties” in our study refers to the estimation in aspects of mangrove ecosystems above ground such as leaf area index (LAI), biomass, carbon, vertical structure, and mangrove health. Understanding these variables is beneficial in detecting the interaction of vegetation, the stability of that interaction, and the change in mangrove population [7,263,274]. Historically, the majority of research on these parameters’ estimation employed ground-based approaches that were time-consuming, costly, and distribute sparsely across space, making regional mangrove monitoring challenging [25]. Alternatively, a number of papers predicted mangrove above-ground properties using vegetation indicators [177,209,220]. These research applied regression analyses to establish empirical relationships between remotely sensed vegetation indices and measured-above ground mangrove (AGM) data (e.g., leaf area index, height canopy, carbon sink, and biomass) [207,209,275,276]. These studies considered that indices derived from satellite data successfully modelled and estimated the mangrove above ground features. However, above ground mangrove ecosystems today have not been compared with the patterns of 30–50 years ago.

In these studies, NDVI and EVI demonstrate the most explanatory curvilinear relationships with AGM [25,65,93]. In fact, there is a saturation issue with NDVI that is mainly due to the red band, the energy in which is strongly absorbed by pigments. When a leaf contains a certain number of pigments, the reflectance remains low and practically constant with more pigment (e.g., increased leaf area) [70,214]. As a result, where forests are high in biomass, NDVI struggles to differentiate moderately high plant cover from very high plant cover [153,214]. Since 2012, most studies confirmed that EVI indicated a higher correlation coefficient with mangrove in field measurements than NDVI to significant extents [59,153,169]. Meanwhile, a few publications found NDVI to be the best mangrove predictor, relative to the performance of EVI and other vegetation indices [80,144,160]. The scale of the analysis also affects the suitability of the index used, with a few studies finding that at a higher resolution (smaller scale) NDVI is the preferred index [84]. In fact, each ecosystem has its unique characteristics, and each index is a separate indication for green vegetation. The best vegetation index to use for AGM estimation varies and thus its selection requires substantial field measurements to validate the results.

4.3. Mangrove Changes

Understanding of variations in mangrove patterns is critical in providing fundamental source for proposing appropriate strategies in mangrove ecosystem management and serving as a reference for broader worldwide applications. The changes in mangrove ecosystems are acknowledged as a result of natural influences and human activities. To investigate mangrove changes, two methodologies are usually applied (i) bi-temporal analysis and (ii) long-term monitoring. Bi-temporal analysis uses two images per 5 or 10 years to assess the changes in mangrove cover. A bi-temporal technique is common and easy to apply, and it calculates the differences of mangrove cover at two times in the context of land use and land cover change. However, there are some limitations in regard to environmental factors (e.g., tide variations, terrain, and atmospheric conditions) if images are only obtained on a single day of the year. This is because we can utilise the method outlined in Section 4.1 to retrieve information about land cover for each year before employing an intersection of two scenes. Besides, the significance of physical factors (e.g., erosion, typhon) as a source of mangrove loss and the trend in mangrove cover may be underestimated.

In contrast, long-term monitoring normally applies time series of spectral indices to understand mangrove dynamics through space and time. Most of studies applied NDVI or EVI and linear regression algorithms to analyse spatiotemporal change and anticipate trends in mangrove distribution at a local scale [172,183,214,277]. These analyses concluded that the loss of mangrove ecosystems is mainly caused by conversion in land use and land cover, compared to natural factors. The aquaculture ponds and impervious surface expansion in the coastal area are a threat to mangrove ecosystems [28]. Globally, Hansen et al. (2013) [277] first used NDVI and ordinary least squares slope of the regression to examine forest loss and gain from 2000 to 2012. The study revealed that a decreased trend in mangrove cover occurred in Asian and Caribbean countries. However, the global analysis overlooked driving factors (e.g., land use and land cover transformation and physical hazards) because policies for land use and land cover changes are different among nations in the world.

Overall, the application of spectral indices for mangrove remote sensing provides several advantages in relation to mapping spatial distribution, above-ground mangrove properties, and mangrove changes. However, examples of knowledge gaps from previous studies should be included (i) visualising mangrove changes from the past to the present; (ii) identifying the driving elements impacting mangroves; and (iii) evaluating effects of environmental factors on satellite images.

5. Discussion and Future Directions

5.1. The Potential Indices for Mangrove Remote Sensing

Over the past 50 years, the importance of spectral indices in mangrove remote sensing has been recognised, but several knowledge gaps still exist in relation to the best index selection for mangrove characterisation. A perfect spectral index for an ensemble of mangrove biophysical parameters is yet to be developed. Our study explored that NDVI accounted for the highest proportion (82%) of the applied spectral indices for mangrove ecosystems, followed by EVI (28%). These normalised algorithms mitigate the atmospheric effects and the impacts of sensor calibration degradation in the red and NIR bands [64,66]. The widespread adoption of remote sensing has resulted in the creation of low-cost image data that may be used to broaden NDVI applications. Hence, NDVI will continue to be a dominant vegetation index used for mangrove remote sensing. However, this does not mean that NDVI is always effective because of its limitations in relation to soil background and vegetation density.

Each index has its own advantages and disadvantages and can be affected by the impacts of the soil background and confounding factors such as sensor and calibration effects, bidirectional reflectance distribution function, atmospheric and topographic effects, or other local environmental conditions (e.g., tide). Hence, for future applications, instead of constructing or discovering a prospective mangrove index, we should examine local conditions and the factors influencing the effectiveness of spectral indices before deciding on the use of them for analysis. Additionally, the number of spectral bands available on optical sensors influenced the indices chosen for mangrove remote sensing. For instance, the four-band version of the Planetscope instrument with no SWIR band is only able to produce spectral indices in the visible and NIR regions. In the case that one index cannot meet the needs of mangrove assessment or other purposes, another index should be applied.

5.2. Long-Term Mangrove Monitoring with Time Series-Based Approaches in Relation to Driving Factors

Monitoring mangrove dynamics normally includes seasonal and annual changes that require a series of historical and regular imagery. In fact, there are many factors, including tide conditions, atmospheric factors, or missing or mis-registered data, that can cause errors in image acquisitions. Therefore, using single-date images to calculate spectral index has shown significant limitations on a large scale because environmental conditions vary from day to day and across sites. Alternatively, generating optical images using averaging is less susceptible to high resolution noise and are thus capable of characterising both long-term and abrupt mangrove changes. For example, using annual mean/median spectral indices that are derived from daily/5-days/8-days/16-days timeseries data enables us to reduce the environmental factors' influence on the image of interest. The study of multiple remotely sensed data has been widely employed in phenological investigations of mangrove ecosystems [121,134,153].

In addition to data, time series analysis provides pieces of information on the timing of mangrove change, as well as improving the quality and accuracy of information being derived using remotely sensed data [167,172,174,217,219]. Also, the time series analysis of spectral indices data evaluates trends and predicts the persistence of mangrove trends under spatial regression application. A variety of time series analysis techniques have been produced [(e.g., National Forest Trend [278], Recurrent Neural Network [279] to analyse and monitor spatiotemporal changes in mangrove ecosystems [191,221,280]. The digital number (DN) value of each pixel from time series images gives more sensitivity than single composited spectral band so that it can easily compare with natural factors (e.g., rainfall, temperature, and ocean dynamics) to certain significance of physical influences. This method holds significant promise for studying the long-term dynamics of environmental variations, and it can monitor future mangrove regeneration.

5.3. Fusion of Images from Multiple Sensors

In the process of the Earth's surface observation and particularly in mangrove remote sensing, selecting a potential optical sensor to calculate spectral index is crucial for assessment with high accuracy. However, there are several factors that can influence the choice of optical remote sensing platforms, such as the purpose of the research, the data availability, the national context, the budget constraints, the scale of the study, and the location of the study area. For instance, to explore spatiotemporal changes in annual mangrove patterns, a long-term time series analysis from Landsat imagery should be preferred because the data is available from 1972 to date. Additionally, to understand mangrove quality or seasonal changes, a variety of MODerate Resolution Imaging Spectroradiometer (MODIS) products with a high temporal resolution (1 day) may be the best choice. Recently, several studies fused multi-sensor images to have more information about mangrove ecosystems. For example, Kanniah et al. (2021) [281] used three optical sensors (i.e., Landsat, MODIS, and Sentinel-2A) to study mangrove fragmentation and health conditions. Guo et al. (2021) [209] used UAV and WorldView-2 datasets to validate the Sentinel-2 imagery for LAI estimation. Besides, several publications fused passive and active sensor images to understand mangrove structure or biomass. Pham et al. (2020) [89] combined optical bands (Sentinel-2A) with active sensors (i.e., Sentinel-1 and ALOS-2 PALSAR-2) to calculate some vegetation indices for mangrove above-ground biomass. These studies concluded that fusing multiple remote sensing sources helps to provide a large amount of information about mangrove ecosystems, compared to single sensor applications.

Fusion of multiple sensors can enhance the accuracy of the data. Integration of NDVI from Advanced Very High-Resolution Radiometer (AVHRR—launched in 1979) and MODIS (launched in the 2000s) enabled a long-term dataset from 1979 to date. AVHRR NDVI composites at 1 km spatial resolution [92,93] was used for mangrove monitoring prior to the 2000s. However, the AVHRR satellite system has degraded in orbit to the point that it is advised that NDVI MODIS products should be used for longer periods in the future [282]. Additionally, combination of ASTER (launched 1999) and Landsat 4, 5, 8, and 9 is an alternative approach for line correction of Landsat 7, allowing us to obtain a set of data at 30 m spatial resolution from 1988 to the present. Notably, using multiple sensors enables improving the re-visit days of satellite data, which is better for smoothing data [25,27]. For example, when Landsat 8 and Landsat 9 are combined, the re-visit days are reduced from 16 to 8 days. Hence, fusion of multiple sensors (i.e., passive, and active sensors) is a recommendable approach to compute the spectral index for mangrove studies in the future.

6. Conclusions

Land use and land cover transformation in relation to natural hazards are the primary factors threatening mangroves in the future. Spectral indices have been applied to mangroves and demonstrated their effectiveness in various studies over 50 years. Each spectral index has its own strength and limitation in mapping mangrove distributions and measuring their above-ground biophysical properties in various environments. Therefore, to select a potential index, we should understand the interaction between the local conditions and mangrove ecosystems. NDVI is the most popular index that can be applied for mangrove ecosystems, followed by EVI, although both are sensitive to environmental conditions.

Long-term mangrove monitoring is crucial for identifying the trend in mangrove pattern changes in connection to driving variables. Using time series analysis of spectral indexes helps to reduce the effect of external influences. Using multiple sensors enables obtaining a set of databases for long-term monitoring associated with natural hazards and human activities. Nowadays, accessing big data has become easier with the help of technology and digital cloud platforms (e.g., Google Earth Engine). These technological advancements will shift mangrove studies from a local to a global scale and imply the necessity to learn programming skills.

In the context of the digital era, mangrove scholars should apply the advantages of cloud computing platforms for spectral index computation. These approaches assist image

processing quickly and enable analysis of mangrove ecosystems at global scale. However, approaching these techniques requests users to have some knowledge about information technology and quite understand about coding. Therefore, developing a tool or application on cloud storage for mangrove monitoring based on vegetation index should be taken into account for new users or scholars who do not have good information technology skills. In addition to tools, a guideline for algorithm selection (e.g., machine learning, deep learning) should be developed to save time for spectral index computation.

Author Contributions: Conceptualization, methodology, formal analysis, investigation, writing—original draft preparation: T.V.T.; writing—review and editing: T.V.T., R.R. and X.Z.; supervision: R.R. and X.Z. All authors have read and agreed to the published version of the manuscript.

Funding: This study was funded by an Australian Research Council Discovery Award DP180103444 to R.R.

Data Availability Statement: The data presented in this study are available on request from the corresponding author.

Acknowledgments: Acknowledgement is given to Monash University for supporting this research. The authors would like to acknowledge the valuable comments of anonymous reviewers and editors that assisted with the finalisation of this manuscript.

Conflicts of Interest: The authors declare no conflict of interest.

Acronyms

EVI	Enhanced Vegetation Index
LAI	Leaf Area Index
NDVI	Normalised Difference Vegetation Index
PVI	Perpendicular Vegetation Index
RVI	Ratio Vegetation Index
SAVI	Soil Adjusted Vegetation Index
TSAVI	Transformed Soil Adjusted Vegetation Index
TVI	Triangular Vegetation Index
VIN	Vegetation Index Number

References

- Tomlinson, P.B. *The Botany of Mangroves*; Cambridge University Press: Cambridge, UK, 2016; ISBN 1-316-79065-7.
- Mandal, R.N.; Bar, R. *Mangroves for Building Resilience to Climate Change*; Apple Academic Press: Waretown, NJ, USA, 2018; ISBN 0-429-48778-9.
- Cavanaugh, K.C.; Osland, M.J.; Bardou, R.; Hinojosa-Arango, G.; López-Vivas, J.M.; Parker, J.D.; Rovai, A.S. Sensitivity of Mangrove Range Limits to Climate Variability. *Glob. Ecol. Biogeogr.* **2018**, *27*, 925–935. [[CrossRef](#)]
- Ellison, A.M.; Farnsworth, E.J.; Merkt, R.E. Origins of Mangrove Ecosystems and the Mangrove Biodiversity Anomaly. *Glob. Ecol. Biogeogr.* **1999**, *8*, 95–115.
- Steenis, C.G.G.J. The Distribution of Mangrove Plant Genera and Its Significance for Palaeogeography. *Proc. Kon. Net. Amst.* **1962**, *65*, 164–169.
- Friess, D.A.; Rogers, K.; Lovelock, C.E.; Krauss, K.W.; Hamilton, S.E.; Lee, S.Y.; Lucas, R.; Primavera, J.; Rajkaran, A.; Shi, S. The State of the World's Mangrove Forests: Past, Present, and Future. *Annu. Rev. Environ. Resour.* **2019**, *44*, 89–115. [[CrossRef](#)]
- Simard, M.; Fatoyinbo, L.; Smetanka, C.; Rivera-Monroy, V.H.; Castañeda-Moya, E.; Thomas, N.; Van der Stocken, T. Mangrove Canopy Height Globally Related to Precipitation, Temperature and Cyclone Frequency. *Nat. Geosci* **2019**, *12*, 40–45. [[CrossRef](#)]
- Kauffman, J.B.; Adame, M.F.; Arifanti, V.B.; Schile-Beers, L.M.; Bernardino, A.F.; Bhomia, R.K.; Donato, D.C.; Feller, I.C.; Ferreira, T.O.; del Carmen Jesus Garcia, M.; et al. Total Ecosystem Carbon Stocks of Mangroves across Broad Global Environmental and Physical Gradients. *Ecol. Monogr.* **2020**, *90*, e01405. [[CrossRef](#)]
- Sandilyan, S.; Kathiresan, K. Mangrove Conservation: A Global Perspective. *Biodivers. Conserv.* **2012**, *21*, 3523–3542. [[CrossRef](#)]
- FAO of the UN. *The World's Mangroves 1980–2005: A Thematic Study Prepared in the Framework of the Global Forest Resources Assessment 2005*; FAO: Rome, Italy, 2007; p. 153.
- Bunting, P.; Rosenqvist, A.; Lucas, R.; Rebelo, L.-M.; Hilarides, L.; Thomas, N.; Hardy, A.; Itoh, T.; Shimada, M.; Finlayson, C. The Global Mangrove Watch—A New 2010 Global Baseline of Mangrove Extent. *Remote Sens.* **2018**, *10*, 1669. [[CrossRef](#)]
- Bunting, P.; Rosenqvist, A.; Hilarides, L.; Lucas, R.M.; Thomas, N. Global Mangrove Watch: Updated 2010 Mangrove Forest Extent (v2. 5). *Remote Sens.* **2022**, *14*, 1034. [[CrossRef](#)]

13. Kuenzer, C.; Bluemel, A.; Gebhardt, S.; Quoc, T.V.; Dech, S. Remote Sensing of Mangrove Ecosystems: A Review. *Remote Sens.* **2011**, *3*, 878–928. [[CrossRef](#)]
14. Lee, S.Y.; Primavera, J.H.; Dahdouh-Guebas, F.; McKee, K.; Bosire, J.O.; Cannicci, S.; Diele, K.; Fromard, F.; Koedam, N.; Marchand, C. Ecological Role and Services of Tropical Mangrove Ecosystems: A Reassessment. *Glob. Ecol. Biogeogr.* **2014**, *23*, 726–743. [[CrossRef](#)]
15. Duke, N.; Nagelkerken, I.; Agardy, T.; Wells, S.; Van Lavieren, H. *The Importance of Mangroves to People: A Call to Action*; United Nations Environment Programme World Conservation Monitoring Centre: Cambridge, UK, 2014; ISBN 92-807-3397-4.
16. Narayan, S.; Beck, M.W.; Reguero, B.G.; Losada, I.J.; Van Wesenbeeck, B.; Pontee, N.; Sanchirico, J.N.; Ingram, J.C.; Lange, G.-M.; Burks-Copes, K.A. The Effectiveness, Costs and Coastal Protection Benefits of Natural and Nature-Based Defences. *PLoS ONE* **2016**, *11*, e0154735. [[CrossRef](#)]
17. Primavera, J.H. Overcoming the Impacts of Aquaculture on the Coastal Zone. *Ocean Coast. Manag.* **2006**, *49*, 531–545. [[CrossRef](#)]
18. Donato, D.C.; Kauffman, J.B.; Mackenzie, R.A.; Ainsworth, A.; Pflieger, A.Z. Whole-Island Carbon Stocks in the Tropical Pacific: Implications for Mangrove Conservation and Upland Restoration. *J. Environ. Manag.* **2012**, *97*, 89–96. [[CrossRef](#)] [[PubMed](#)]
19. Donato, D.C.; Kauffman, J.B.; Murdiyarto, D.; Kurnianto, S.; Stidham, M.; Kanninen, M. Mangroves among the Most Carbon-Rich Forests in the Tropics. *Nat. Geosci.* **2011**, *4*, 293–297. [[CrossRef](#)]
20. Spalding, M.; Parrett, C.L. Global Patterns in Mangrove Recreation and Tourism. *Mar. Policy* **2019**, *110*, 103540. [[CrossRef](#)]
21. Giri, C.; Ochieng, E.; Tieszen, L.L.; Zhu, Z.; Singh, A.; Loveland, T.; Masek, J.; Duke, N. Status and Distribution of Mangrove Forests of the World Using Earth Observation Satellite Data. *Glob. Ecol. Biogeogr.* **2011**, *20*, 154–159. [[CrossRef](#)]
22. Carugati, L.; Gatto, B.; Rastelli, E.; Lo Martire, M.; Coral, C.; Greco, S.; Danovaro, R. Impact of Mangrove Forests Degradation on Biodiversity and Ecosystem Functioning. *Sci. Rep.* **2018**, *8*, 13298. [[CrossRef](#)]
23. Goldberg, L.; Lagomasino, D.; Thomas, N.; Fatoyinbo, T. Global Declines in Human-Driven Mangrove Loss. *Glob. Change Biol.* **2020**, *26*, 5844–5855. [[CrossRef](#)]
24. Su, J.; Friess, D.A.; Gasparatos, A. A Meta-Analysis of the Ecological and Economic Outcomes of Mangrove Restoration. *Nat. Commun.* **2021**, *12*, 5050. [[CrossRef](#)]
25. Wang, L.; Jia, M.; Yin, D.; Tian, J. A Review of Remote Sensing for Mangrove Forests: 1956–2018. *Remote Sens. Environ.* **2019**, *231*, 111223. [[CrossRef](#)]
26. Pham, T.D.; Yokoya, N.; Bui, D.T.; Yoshino, K.; Friess, D.A. Remote Sensing Approaches for Monitoring Mangrove Species, Structure, and Biomass: Opportunities and Challenges. *Remote Sens.* **2019**, *11*, 230. [[CrossRef](#)]
27. Maurya, K.; Mahajan, S.; Chaube, N. Remote Sensing Techniques: Mapping and Monitoring of Mangrove Ecosystem—A Review. *Complex Intell. Syst.* **2021**, *7*, 2797–2818. [[CrossRef](#)]
28. Cardenas, N.Y.; Joyce, K.E.; Maier, S.W. Monitoring Mangrove Forests: Are We Taking Full Advantage of Technology? *Int. J. Appl. Earth Obs. Geoinf.* **2017**, *63*, 1–14.
29. Campbell, J.B.; Wynne, R.H. *Introduction to Remote Sensing*; Guilford Press: New York, NY, USA, 2011; ISBN 1-60918-177-8.
30. Thakur, S.; Mondal, I.; Ghosh, P.B.; Das, P.; De, T.K. A Review of the Application of Multispectral Remote Sensing in the Study of Mangrove Ecosystems with Special Emphasis on Image Processing Techniques. *Spat. Inf. Res.* **2020**, *28*, 39–51. [[CrossRef](#)]
31. Zulfa, A.W.; Norizah, K.; Hamdan, O.; Faridah-Hanum, I.; Rhyma, P.P.; Fitrianto, A. Spectral Signature Analysis to Determine Mangrove Species Delineation Structured by Anthropogenic Effects. *Ecol. Indic.* **2021**, *130*, 108148. [[CrossRef](#)]
32. Zulfa, A.W.; Norizah, K.; Hamdan, O.; Zulkifly, S.; Faridah-Hanum, I.; Rhyma, P.P. Discriminating Trees Species from the Relationship between Spectral Reflectance and Chlorophyll Contents of Mangrove Forest in Malaysia. *Ecol. Indic.* **2020**, *111*, 106024. [[CrossRef](#)]
33. Green, E.P.; Clark, C.D.; Mumby, P.J.; Edwards, A.J.; Ellis, A.C. Remote Sensing Techniques for Mangrove Mapping. *Int. J. Remote Sens.* **1998**, *19*, 935–956. [[CrossRef](#)]
34. Heumann, B.W. Satellite Remote Sensing of Mangrove Forests: Recent Advances and Future Opportunities. *Prog. Phys. Geogr.* **2011**, *35*, 87–108. [[CrossRef](#)]
35. Purnamasayangasukasih, P.R.; Norizah, K.; Ismail, A.A.; Shamsudin, I. A Review of Uses of Satellite Imagery in Monitoring Mangrove Forests. In Proceedings of the IOP Conference Series: Earth and Environmental Science; IOP Publishing: Bristol, UK, 2016; Volume 37, p. 012034.
36. Estes, J.; Kline, K.; Collins, E. Remote Sensing. In *International Encyclopedia of the Social & Behavioral Sciences*; Smelser, N.J., Baltes, P.B., Eds.; Pergamon: Oxford, UK, 2001; pp. 13144–13150. ISBN 978-0-08-043076-8.
37. Pricope, N.G.; Mapes, K.L.; Woodward, K.D. Remote Sensing of Human–Environment Interactions in Global Change Research: A Review of Advances, Challenges and Future Directions. *Remote Sens.* **2019**, *11*, 2783. [[CrossRef](#)]
38. Aria, M.; Cuccurullo, C. Bibliometrix: An R-Tool for Comprehensive Science Mapping Analysis. *J. Informetr.* **2017**, *11*, 959–975. [[CrossRef](#)]
39. Derviş, H. Bibliometric Analysis Using Bibliometrix an R Package. *J. Scientometr. Res.* **2019**, *8*, 156–160. [[CrossRef](#)]
40. Aria, M.; Misuraca, M.; Spano, M. Mapping the Evolution of Social Research and Data Science on 30 Years of Social Indicators Research. *Soc. Indic. Res.* **2020**, *149*, 803–831. [[CrossRef](#)]
41. Duan, P.; Wang, Y.; Yin, P. Remote Sensing Applications in Monitoring of Protected Areas: A Bibliometric Analysis. *Remote Sens.* **2020**, *12*, 772. [[CrossRef](#)]

42. Prancutė, R. Web of Science (WoS) and Scopus: The Titans of Bibliographic Information in Today's Academic World. *Publications* **2021**, *9*, 12. [[CrossRef](#)]
43. Zhu, J.; Liu, W. A Tale of Two Databases: The Use of Web of Science and Scopus in Academic Papers. *Scientometrics* **2020**, *123*, 321–335. [[CrossRef](#)]
44. Aghaei Chadegani, A.; Salehi, H.; Yunus, M.; Farhadi, H.; Fooladi, M.; Farhadi, M.; Ale Ebrahim, N. *A Comparison between Two Main Academic Literature Collections: Web of Science and Scopus Databases*; Social Science Research Network: Rochester, NY, USA, 2013.
45. Moral-Muñoz, J.A.; Herrera-Viedma, E.; Santisteban-Espejo, A.; Cobo, M.J. Software Tools for Conducting Bibliometric Analysis in Science: An up-to-Date Review. *Prof. Inf.* **2020**, *29*, e290103. [[CrossRef](#)]
46. Clarivate, A. Web of Science Journal Evaluation Process and Selection Criteria. Available online: <https://clarivate.com/webofsciencelibrary/journal-evaluation-process-and-selection-criteria/> (accessed on 7 February 2022).
47. Shu, F. Research on the Application of Thomson Data Analyzer to Analyses the Patent Intelligence of Scientific Institutions. *Inf. Sci.* **2008**, *26*, 1833–1843.
48. Perianes-Rodriguez, A.; Waltman, L.; van Eck, N.J. Constructing Bibliometric Networks: A Comparison between Full and Fractional Counting. *J. Informetr.* **2016**, *10*, 1178–1195. [[CrossRef](#)]
49. Liu, W. The Data Source of This Study Is Web of Science Core Collection? Not Enough. *Scientometrics* **2019**, *121*, 1815–1824. [[CrossRef](#)]
50. Bannari, A.; Morin, D.; Bonn, F.; Huete, A.R. A Review of Vegetation Indices. *Remote Sens. Rev.* **1995**, *13*, 95–120. [[CrossRef](#)]
51. Raynaud, M.; Goutaudier, V.; Louis, K.; Al-Awadhi, S.; Dubourg, Q.; Truchot, A.; Brousse, R.; Saleh, N.; Giarraputo, A.; Debiais, C.; et al. Impact of the COVID-19 Pandemic on Publication Dynamics and Non-COVID-19 Research Production. *BMC Med. Res. Methodol.* **2021**, *21*, 255. [[CrossRef](#)] [[PubMed](#)]
52. Vinay, V.; Julia, L. Introducing the Spectral Index Library in ArcGIS. Available online: <https://www.esri.com/about/newsroom/arcuser/spectral-library/> (accessed on 6 February 2022).
53. Xue, J.; Su, B. Significant Remote Sensing Vegetation Indices: A Review of Developments and Applications. *J. Sens.* **2017**, *2017*, 1353691. [[CrossRef](#)]
54. Deng, Y.; Wu, C.; Li, M.; Chen, R. RNDISI: A Ratio Normalized Difference Soil Index for Remote Sensing of Urban/Suburban Environments. *Int. J. Appl. Earth Obs. Geoinf.* **2015**, *39*, 40–48. [[CrossRef](#)]
55. Baloloy, A.B.; Blanco, A.C.; Sta, A.R.R.C.; Nadaoka, K. Development and Application of a New Mangrove Vegetation Index (MVI) for Rapid and Accurate Mangrove Mapping. *ISPRS J. Photogramm. Remote Sens.* **2020**, *166*, 95–117. [[CrossRef](#)]
56. Winarso, G.; Purwanto, A.; Yuwono, D.; Center, R.S.A. New Mangrove Index as Degradation Health Indicator Using Remote Sensing Data: Segara Anakan and Alas Purwo Case Study. In Proceedings of the 12th Biennial Conference of Pan Ocean Remote Sensing Conference (PORSEC 2014), Bali, Indonesia, 4–7 November 2014; pp. 4–7.
57. Zhang, X.; Tian, Q. A Mangrove Recognition Index for Remote Sensing of Mangrove Forest from Space. *Curr. Sci.* **2013**, *105*, 1149–1154.
58. Gupta, K.; Mukhopadhyay, A.; Giri, S.; Chanda, A.; Majumdar, S.D.; Samanta, S.; Mitra, D.; Samal, R.N.; Pattnaik, A.K.; Hazra, S. An Index for Discrimination of Mangroves from Non-Mangroves Using LANDSAT 8 OLI Imagery. *MethodsX* **2018**, *5*, 1129–1139. [[CrossRef](#)]
59. Kumar, A.; Stupp, P.; Dahal, S.; Remillard, C.; Bledsoe, R.; Stone, A.; Cameron, C.; Rastogi, G.; Samal, R.; Mishra, D.R. A Multi-Sensor Approach for Assessing Mangrove Biophysical Characteristics in Coastal Odisha, India. *Proc. Natl. Acad. Sci. USA India Sect. A Phys. Sci.* **2017**, *87*, 679–700. [[CrossRef](#)]
60. Jia, M.; Wang, Z.; Wang, C.; Mao, D.; Zhang, Y. A New Vegetation Index to Detect Periodically Submerged Mangrove Forest Using Single-Tide Sentinel-2 Imagery. *Remote Sens.* **2019**, *11*, 2043. [[CrossRef](#)]
61. McFeeters, S.K. The Use of the Normalized Difference Water Index (NDWI) in the Delineation of Open Water Features. *Int. J. Remote Sens.* **1996**, *17*, 1425–1432. [[CrossRef](#)]
62. Pearson, R.L.; Miller, L.D. Remote Mapping of Standing Crop Biomass for Estimation of the Productivity of the Shortgrass Prairie. *Remote Sens. Environ.* **1972**, *8*, 1355–1379.
63. Rouse, J.W.; Haas, R.H.; Schell, J.A.; Deering, D.W. Monitoring Vegetation Systems in the Great Plains with ERTS. In *Third Earth Reserves Technology Satellite Symposium*; Greenbelt: NASA SP-351; NASA: Washington, DC, USA, 1973; Volume 30103017, pp. 309–317.
64. Huang, S.; Tang, L.; Hupy, J.P.; Wang, Y.; Shao, G. A Commentary Review on the Use of Normalized Difference Vegetation Index (NDVI) in the Era of Popular Remote Sensing. *J. For. Res.* **2021**, *32*, 1–6. [[CrossRef](#)]
65. Jensen, J.R.; Lin, H.; Yang, X.; Ramsey, E., III; Davis, B.A.; Thoenke, C.W. The Measurement of Mangrove Characteristics in Southwest Florida Using SPOT Multispectral Data. *Geocarto Int.* **1991**, *6*, 13–21. [[CrossRef](#)]
66. Forkel, M.; Carvalhais, N.; Verbesselt, J.; Mahecha, M.D.; Neigh, C.S.R.; Reichstein, M. Trend Change Detection in NDVI Time Series: Effects of Inter-Annual Variability and Methodology. *Remote Sens.* **2013**, *5*, 2113–2144. [[CrossRef](#)]
67. Huete, A.R. A Soil-Adjusted Vegetation Index (SAVI). *Remote Sens. Environ.* **1988**, *25*, 295–309. [[CrossRef](#)]
68. Baret, F.; Guyot, G.; Major, D.J. TSAVI: A Vegetation Index Which Minimizes Soil Brightness Effects on LAI and APAR Estimation. In Proceedings of the 12th Canadian Symposium on Remote Sensing Geoscience and Remote Sensing Symposium, Vancouver, BC, Canada, 10–14 July 1989; Volume 3, pp. 1355–1358.

69. Huete, A.; Didan, K.; Miura, T.; Rodriguez, E.P.; Gao, X.; Ferreira, L.G. Overview of the Radiometric and Biophysical Performance of the MODIS Vegetation Indices. *Remote Sens. Environ.* **2002**, *83*, 195–213. [[CrossRef](#)]
70. Tran, T.V.; Tran, D.X.; Nguyen, H.; Latorre-Carmona, P.; Myint, S.W. Characterising Spatiotemporal Vegetation Variations Using LANDSAT Time-Series and Hurst Exponent Index in the Mekong River Delta. *Land Degrad. Dev.* **2021**, *32*, 3507–3523. [[CrossRef](#)]
71. Jiang, Z.; Huete, A.R.; Didan, K.; Miura, T. Development of a Two-Band Enhanced Vegetation Index without a Blue Band. *Remote Sens. Environ.* **2008**, *112*, 3833–3845. [[CrossRef](#)]
72. Liu, H.Q.; Huete, A. A Feedback Based Modification of the NDVI to Minimize Canopy Background and Atmospheric Noise. *IEEE Trans. Geosci. Remote Sens.* **1995**, *33*, 457–465. [[CrossRef](#)]
73. Richardson, A.J.; Wiegand, C.L. Distinguishing Vegetation from Soil Background Information. *Photogramm. Eng. Remote Sens.* **1977**, *43*, 1541–1552.
74. Wicaksono, P.; Danoedoro, P.; Hartono; Nehren, U. Mangrove Biomass Carbon Stock Mapping of the Karimunjawa Islands Using Multispectral Remote Sensing. *Int. J. Remote Sens.* **2015**, *37*, 26–52. [[CrossRef](#)]
75. Wicaksono, P. Mangrove Above-Ground Carbon Stock Mapping of Multi-Resolution Passive Remote-Sensing Systems. *Int. J. Remote Sens.* **2017**, *38*, 1551–1578. [[CrossRef](#)]
76. Diaz, B.M.; Blackburn, G.A. Remote Sensing of Mangrove Biophysical Properties: Evidence from a Laboratory Simulation of the Possible Effects of Background Variation on Spectral Vegetation Indices. *Int. J. Remote Sens.* **2003**, *24*, 53–73. [[CrossRef](#)]
77. Kovacs, J.M.; Flores-Verdugo, F.; Wang, J.; Aspden, L.P. Estimating Leaf Area Index of a Degraded Mangrove Forest Using High Spatial Resolution Satellite Data. *Aquat. Bot.* **2004**, *80*, 13–22. [[CrossRef](#)]
78. Kovacs, J.M.; King, J.M.L.; Flores de Santiago, F.; Flores-Verdugo, F. Evaluating the Condition of a Mangrove Forest of the Mexican Pacific Based on an Estimated Leaf Area Index Mapping Approach. *Environ. Monit Assess* **2009**, *157*, 137–149. [[CrossRef](#)]
79. Kovacs, J.M.; Liu, Y.; Zhang, C.; Flores-Verdugo, F.; de Santiago, F.F. A Field Based Statistical Approach for Validating a Remotely Sensed Mangrove Forest Classification Scheme. *Wetl. Ecol. Manag.* **2011**, *19*, 409. [[CrossRef](#)]
80. Kamal, M.; Phinn, S.; Johansen, K. Assessment of Multi-Resolution Image Data for Mangrove Leaf Area Index Mapping. *Remote Sens. Environ.* **2016**, *176*, 242–254. [[CrossRef](#)]
81. Heenkenda, M.K.; Maier, S.W.; Joyce, K.E. Estimating Mangrove Biophysical Variables Using WorldView-2 Satellite Data: Rapid Creek, Northern Territory, Australia. *J. Imaging* **2016**, *2*, 24. [[CrossRef](#)]
82. Zhu, Y.; Liu, K.; Liu, L.; Myint, S.W.; Wang, S.; Liu, H.; He, Z. Exploring the Potential of WorldView-2 Red-Edge Band-Based Vegetation Indices for Estimation of Mangrove Leaf Area Index with Machine Learning Algorithms. *Remote Sens.* **2017**, *9*, 1060. [[CrossRef](#)]
83. George, R.; Padalia, H.; Sinha, S.K.; Kumar, A.S. Evaluation of the Use of Hyperspectral Vegetation Indices for Estimating Mangrove Leaf Area Index in Middle Andaman Island, India. *Remote Sens. Lett.* **2018**, *9*, 1099–1108. [[CrossRef](#)]
84. Wicaksono, P.; Hafizt, M. Dark Target Effectiveness for Dark-Object Subtraction Atmospheric Correction Method on Mangrove above-Ground Carbon Stock Mapping. *IET Image Processing* **2018**, *12*, 582–587. [[CrossRef](#)]
85. Muhsoni, F.F.; Sambah, A.B.; Mahmudi, M.; Wiadnya, D.G.R. Estimation of Mangrove Carbon Stock with Hybrid Method Using Image Sentinel-2. *GEOMATE J.* **2018**, *15*, 185–192. [[CrossRef](#)]
86. Oostdijk, M.; Santos, M.J.; Whigham, D.; Verhoeven, J.; Silvestri, S. Assessing Rehabilitation of Managed Mangrove Ecosystems Using High Resolution Remote Sensing. *Estuar. Coast. Shelf Sci.* **2018**, *211*, 238–247. [[CrossRef](#)]
87. Razali, S.M.; Nuruddin, A.A.; Kamarudin, N. Mapping Mangrove Density for Conservation of the RAMSAR Site in Peninsular Malaysia. *Int. J. Conserv. Sci.* **2020**, *11*, 153–164.
88. Ávila-Flores, G.; Juárez-Mancilla, J.; Hinojosa-Arango, G.; Cruz-Chávez, P.; López-Vivas, J.M.; Arizpe-Covarrubias, O. A Practical Index to Estimate Mangrove Conservation Status: The Forests from La Paz Bay, Mexico as a Case Study. *Sustainability* **2020**, *12*, 858. [[CrossRef](#)]
89. Pham, T.D.; Yokoya, N.; Xia, J.; Ha, N.T.; Le, N.N.; Nguyen, T.T.T.; Dao, T.H.; Vu, T.T.P.; Pham, T.D.; Takeuchi, W. Comparison of Machine Learning Methods for Estimating Mangrove Above-Ground Biomass Using Multiple Source Remote Sensing Data in the Red River Delta Biosphere Reserve, Vietnam. *Remote Sens.* **2020**, *12*, 1334. [[CrossRef](#)]
90. Xia, Q.; Qin, C.-Z.; Li, H.; Huang, C.; Su, F.-Z.; Jia, M.-M. Evaluation of Submerged Mangrove Recognition Index Using Multi-Tidal Remote Sensing Data. *Ecol. Indic.* **2020**, *113*, 106196. [[CrossRef](#)]
91. Ali, A.; Nayyar, Z.A. Extraction of Mangrove Forest through Landsat 8 Mangrove Index (L8MI). *Arab. J. Geosci.* **2020**, *13*, 1132. [[CrossRef](#)]
92. Ramsey, E.W.R., III; Jensen, J.R. Remote Sensing of Mangrove Wetlands: Relating Canopy Spectra to Site-Specific Data. *Photogramm. Eng. Remote Sens.* **1996**, *62*, 939–948.
93. Green, E.P.; Mumby, P.J.; Edwards, A.J.; Clark, C.D.; Ellis, A.C. Estimating Leaf Area Index of Mangroves from Satellite Data. *Aquat. Bot.* **1997**, *58*, 11–19. [[CrossRef](#)]
94. Green, E.; Mumby, P.; Edwards, A.; Clark, C.; Ellis, A. The Assessment of Mangrove Areas Using High Resolution Multispectral Airborne Imagery. *J. Coast. Res.* **1998**, *14*, 433–443.
95. Ruiz-Luna, A.; Berlanga-Robles, C. Modifications in Coverage Patterns and Land Use around the Huizache-Caimanero Lagoon System, Sinaloa, Mexico: A Multi-Temporal Analysis Using LANDSAT Images. *Estuar. Coast. Shelf Sci.* **1999**, *49*, 37–44. [[CrossRef](#)]
96. Kovacs, J.M.; Wang, J.; Flores-Verdugo, F. Mapping Mangrove Leaf Area Index at the Species Level Using IKONOS and LAI-2000 Sensors for the Agua Brava Lagoon, Mexican Pacific. *Estuar. Coast. Shelf Sci.* **2005**, *62*, 377–384. [[CrossRef](#)]

97. Mantri, V.A.; Mishra, A.K. On Monitoring Mangrove Vegetation of Sagar Island by Remote Sensing. *Natl. Acad. Sci. Lett.* **2006**, *29*, 45–48. [[CrossRef](#)]
98. Nichol, C.J.; Rascher, U.; Matsubara, S.; Osmond, B. Assessing Photosynthetic Efficiency in an Experimental Mangrove Canopy Using Remote Sensing and Chlorophyll Fluorescence. *Trees* **2005**, *20*, 9. [[CrossRef](#)]
99. Li, X.; Gar-On Yeh, A.; Wang, S.; Liu, K.; Liu, X.; Qian, J.; Chen, X. Regression and Analytical Models for Estimating Mangrove Wetland Biomass in South China Using Radarsat Images. *Int. J. Remote Sens.* **2007**, *28*, 5567–5582. [[CrossRef](#)]
100. Kovacs, J.M.; Zhang, C.; Flores-Verdugo, F.J. Mapping the Condition of Mangroves of the Mexican Pacific Using C-Band ENVISAT ASAR and Landsat Optical Data. *Cienc. Mar.* **2008**, *34*, 407–418. [[CrossRef](#)]
101. Lee, T.-M.; Yeh, H.-C. Applying Remote Sensing Techniques to Monitor Shifting Wetland Vegetation: A Case Study of Danshui River Estuary Mangrove Communities, Taiwan. *Ecol. Eng.* **2009**, *35*, 487–496. [[CrossRef](#)]
102. Rajitha, K.; Mukherjee, C.K.; Vinu Chandran, R.; Prakash Mohan, M.M. Land-Cover Change Dynamics and Coastal Aquaculture Development: A Case Study in the East Godavari Delta, Andhra Pradesh, India Using Multi-Temporal Satellite Data. *Int. J. Remote Sens.* **2010**, *31*, 4423–4442. [[CrossRef](#)]
103. Ruiz-Luna, A.; Cervantes Escobar, A.; Berlanga-Robles, C. Assessing Distribution Patterns, Extent, and Current Condition of Northwest Mexico Mangroves. *Wetlands* **2010**, *30*, 717–723. [[CrossRef](#)]
104. Satyanarayana, B.; Mohamad, K.A.; Idris, I.F.; Husain, M.-L.; Dahdouh-Guebas, F. Assessment of Mangrove Vegetation Based on Remote Sensing and Ground-Truth Measurements at Tumpat, Kelantan Delta, East Coast of Peninsular Malaysia. *Int. J. Remote Sens.* **2011**, *32*, 1635–1650. [[CrossRef](#)]
105. Kamthonkiat, D.; Rodfai, C.; Saiwanrungskul, A.; Koshimura, S.; Matsuoka, M. Geoinformatics in Mangrove Monitoring: Damage and Recovery after the 2004 Indian Ocean Tsunami in Phang Nga, Thailand. *Nat. Hazards Earth Syst. Sci.* **2011**, *11*, 1851–1862. [[CrossRef](#)]
106. Pujiono, E.; Kwak, D.-A.; Lee, W.-K.; Sulistyanto; Kim, S.-R.; Lee, J.Y.; Lee, S.-H.; Park, T.; Kim, M.-I. RGB-NDVI Color Composites for Monitoring the Change in Mangrove Area at the Maubesi Nature Reserve, Indonesia. *For. Sci. Technol.* **2013**, *9*, 171–179. [[CrossRef](#)]
107. Vo, Q.T.; Oppelt, N.; Leinenkugel, P.; Kuenzer, C. Remote Sensing in Mapping Mangrove Ecosystems—An Object-Based Approach. *Remote Sens.* **2013**, *5*, 183–201. [[CrossRef](#)]
108. Wong, F.K.K.; Fung, T. Combining Hyperspectral and Radar Imagery for Mangrove Leaf Area Index Modeling. *Photogramm. Eng. Remote Sens.* **2013**, *79*, 479–490. [[CrossRef](#)]
109. Manna, S.; Mondal, P.P.; Mukhopadhyay, A.; Akhand, A.; Hazra, S.; Mitra, D. Vegetation Cover Change Analysis from Multi-Temporal Satellite Data in Jharkhali Island, Sundarbans, India. *IJMS* **2013**, *42*, 331–342.
110. Hamdan, O.; Khairunnisa, M.; Ammar, A.; Hasmadi, I.M.; Aziz, H.K. Mangrove Carbon Stock Assessment by Optical Satellite Imagery. *J. Trop. For. Sci.* **2013**, *25*, 554–565.
111. Wohlfart, C.; Wegmann, M.; Leimgruber, P. Mapping Threatened Dry Deciduous Dipterocarp Forest in South-East Asia for Conservation Management. *Trop. Conserv. Sci.* **2014**, *7*, 597–613. [[CrossRef](#)]
112. Almeida, P.; Altobelli, A.; D'Aiotti, L.; Feoli, E.; Ganis, P.; Giordano, F.; Napolitano, R.; Simonetti, C. The Role of Vegetation Analysis by Remote Sensing and GIS Technology for Planning Sustainable Development: A Case Study for the Santos Estuary Drainage Basin (Brazil). *Plant Biosyst.-Int. J. Deal. All Asp. Plant Biol.* **2014**, *148*, 540–546. [[CrossRef](#)]
113. Fuller, D.; Wang, Y. Recent Trends in Satellite Vegetation Index Observations Indicate Decreasing Vegetation Biomass in the Southeastern Saline Everglades Wetlands. *Wetlands* **2014**, *34*, 67–77. [[CrossRef](#)]
114. Chellamani, P.; Singh, C.P.; Panigrahy, S. Assessment of the Health Status of Indian Mangrove Ecosystems Using Multi Temporal Remote Sensing Data. *Trop. Ecol.* **2014**, *55*, 245–253.
115. Manna, S.; Nandy, S.; Chanda, A.; Akhand, A.; Hazra, S.; Dadhwal, V.K. Estimating Aboveground Biomass in Avicennia Marina Plantation in Indian Sundarbans Using High-Resolution Satellite Data. *J. Appl. Remote Sens.* **2014**, *8*, 083638. [[CrossRef](#)]
116. Anwar, M.S.; Takewaka, S. Analyses on Phenological and Morphological Variations of Mangrove Forests along the Southwest Coast of Bangladesh. *J. Coast. Conserv.* **2014**, *18*, 339–357. [[CrossRef](#)]
117. Patil, V.; Singh, A.; Naik, N.; Unnikrishnan, S. Estimation of Mangrove Carbon Stocks by Applying Remote Sensing and GIS Techniques. *Wetlands* **2015**, *35*, 695–707. [[CrossRef](#)]
118. Ibharm, N.A.; Mustapha, M.A.; Lihan, T.; Mazlan, A.G. Mapping Mangrove Changes in the Matang Mangrove Forest Using Multi Temporal Satellite Imageries. *Ocean Coast. Manag.* **2015**, *114*, 64–76. [[CrossRef](#)]
119. Heenkenda, M.K.; Joyce, K.E.; Maier, S.W.; de Bruin, S. Quantifying Mangrove Chlorophyll from High Spatial Resolution Imagery. *ISPRS J. Photogramm. Remote Sens.* **2015**, *108*, 234–244. [[CrossRef](#)]
120. Lagomasino, D.; Price, R.M.; Whitman, D.; Melesse, A.; Oberbauer, S.F. Spatial and Temporal Variability in Spectral-Based Surface Energy Evapotranspiration Measured from Landsat 5TM across Two Mangrove Ecotones. *Agric. For. Meteorol.* **2015**, *213*, 304–316. [[CrossRef](#)]
121. Alatorre, L.C.; Sánchez-Carrillo, S.; Miramontes-Beltrán, S.; Medina, R.J.; Torres-Olave, M.E.; Bravo, L.C.; Wiebe, L.C.; Granados, A.; Adams, D.K.; Sánchez, E.; et al. Temporal Changes of NDVI for Qualitative Environmental Assessment of Mangroves: Shrimp Farming Impact on the Health Decline of the Arid Mangroves in the Gulf of California (1990–2010). *J. Arid Environ.* **2016**, *125*, 98–109. [[CrossRef](#)]

122. Jana, A.; Maiti, S.; Biswas, A. Seasonal Change Monitoring and Mapping of Coastal Vegetation Types along Midnapur-Balasore Coast, Bay of Bengal Using Multi-Temporal Landsat Data. *Model. Earth Syst. Environ.* **2015**, *2*, 7. [[CrossRef](#)]
123. Zhang, K.; Thapa, B.; Ross, M.; Gann, D. Remote Sensing of Seasonal Changes and Disturbances in Mangrove Forest: A Case Study from South Florida. *Ecosphere* **2016**, *7*, e01366. [[CrossRef](#)]
124. Conti, L.A.; de Araújo, C.A.S.; Cunha-Lignon, M. Spatial Database Modeling for Mangrove Forests Mapping; Example of Two Estuarine Systems in Brazil. *Model. Earth Syst. Environ.* **2016**, *2*, 73. [[CrossRef](#)]
125. Rodriguez, W.; Feller, I.C.; Cavanaugh, K.C. Spatio-Temporal Changes of a Mangrove–Saltmarsh Ecotone in the Northeastern Coast of Florida, USA. *Glob. Ecol. Conserv.* **2016**, *7*, 245–261. [[CrossRef](#)]
126. Malone, S.L.; Barr, J.; Fuentes, J.D.; Oberbauer, S.F.; Staudhammer, C.L.; Gaiser, E.E.; Starr, G. Sensitivity to Low-Temperature Events: Implications for CO₂ Dynamics in Subtropical Coastal Ecosystems. *Wetlands* **2016**, *36*, 957–967. [[CrossRef](#)]
127. Nardin, W.; Locatelli, S.; Pasquarella, V.; Rulli, M.C.; Woodcock, C.E.; Fagherazzi, S. Dynamics of a Fringe Mangrove Forest Detected by Landsat Images in the Mekong River Delta, Vietnam. *Earth Surf. Process. Landf.* **2016**, *41*, 2024–2037. [[CrossRef](#)]
128. Son, N.-T.; Chen, C.-F.; Chen, C.-R. Mapping Mangrove Density from Rapideye Data in Central America. *Open Geosci.* **2017**, *9*, 211–220. [[CrossRef](#)]
129. Yagci, A.L.; Santanello, J.A.; Jones, J.W.; Barr, J. Estimating Evaporative Fraction from Readily Obtainable Variables in Mangrove Forests of the Everglades, U.S.A. *Int. J. Remote Sens.* **2017**, *38*, 3981–4007. [[CrossRef](#)]
130. Abd-El Monsef, H.; Smith, S.E. A New Approach for Estimating Mangrove Canopy Cover Using Landsat 8 Imagery. *Comput. Electron. Agric.* **2017**, *135*, 183–194. [[CrossRef](#)]
131. Lovelock, C.E.; Feller, I.C.; Reef, R.; Hickey, S.; Ball, M.C. Mangrove Dieback during Fluctuating Sea Levels. *Sci. Rep.* **2017**, *7*, 1680. [[CrossRef](#)]
132. Pham, L.T.; Brabyn, L. Monitoring Mangrove Biomass Change in Vietnam Using SPOT Images and an Object-Based Approach Combined with Machine Learning Algorithms. *ISPRS J. Photogramm. Remote Sens.* **2017**, *128*, 86–97. [[CrossRef](#)]
133. Tian, J.; Wang, L.; Li, X.; Gong, H.; Shi, C.; Zhong, R.; Liu, X. Comparison of UAV and WorldView-2 Imagery for Mapping Leaf Area Index of Mangrove Forest. *Int. J. Appl. Earth Obs. Geoinf.* **2017**, *61*, 22–31. [[CrossRef](#)]
134. Chen, B.; Xiao, X.; Li, X.; Pan, L.; Doughty, R.; Ma, J.; Dong, J.; Qin, Y.; Zhao, B.; Wu, Z. A Mangrove Forest Map of China in 2015: Analysis of Time Series Landsat 7/8 and Sentinel-1A Imagery in Google Earth Engine Cloud Computing Platform. *ISPRS J. Photogramm. Remote Sens.* **2017**, *131*, 104–120. [[CrossRef](#)]
135. Zhang, X.; Treitz, P.M.; Chen, D.; Quan, C.; Shi, L.; Li, X. Mapping Mangrove Forests Using Multi-Tidal Remotely-Sensed Data and a Decision-Tree-Based Procedure. *Int. J. Appl. Earth Obs. Geoinf.* **2017**, *62*, 201–214. [[CrossRef](#)]
136. Castillo, J.A.A.; Apan, A.A.; Maraseni, T.N.; Salmo, S.G. Estimation and Mapping of Above-Ground Biomass of Mangrove Forests and Their Replacement Land Uses in the Philippines Using Sentinel Imagery. *ISPRS J. Photogramm. Remote Sens.* **2017**, *134*, 70–85. [[CrossRef](#)]
137. Galeano, A.; Urrego, L.E.; Botero, V.; Bernal, G. Mangrove Resilience to Climate Extreme Events in a Colombian Caribbean Island. *Wetl. Ecol. Manag.* **2017**, *25*, 743–760. [[CrossRef](#)]
138. Milani, A.S. Mangrove Forests of the Persian Gulf and the Gulf of Oman. In *Threats to Mangrove Forests: Hazards, Vulnerability, and Management*; Makowski, C., Finkl, C.W., Eds.; Coastal Research Library; Springer International Publishing: Cham, Switzerland, 2018; pp. 53–75. ISBN 978-3-319-73016-5.
139. Muhd-Ekhzarizal, M.; Mohd-Hasnadi, I.; Hamdan, O.; Mohamad-Roslan, M.; Noor-Shaila, S. Estimation of Aboveground Biomass in Mangrove Forests Using Vegetation Indices from SPOT-5 Image. *J. Trop. For. Sci.* **2018**, *30*, 224–233.
140. Valderrama-Landeros, L.; Flores-de-Santiago, F.; Kovacs, J.M.; Flores-Verdugo, F. An Assessment of Commonly Employed Satellite-Based Remote Sensors for Mapping Mangrove Species in Mexico Using an NDVI-Based Classification Scheme. *Environ. Monit. Assess* **2018**, *190*, 23. [[CrossRef](#)]
141. Flores-Cárdenas, F.; Millán-Aguilar, O.; Díaz-Lara, L.; Rodríguez-Arredondo, L.; Hurtado-Oliva, M.Á.; Manzano-Sarabia, M. Trends in the Normalized Difference Vegetation Index for Mangrove Areas in Northwestern Mexico. *J. Coast. Res.* **2018**, *34*, 877–882. [[CrossRef](#)]
142. Wang, M.; Cao, W.; Guan, Q.; Wu, G.; Wang, F. Assessing Changes of Mangrove Forest in a Coastal Region of Southeast China Using Multi-Temporal Satellite Images. *Estuar. Coast. Shelf Sci.* **2018**, *207*, 283–292. [[CrossRef](#)]
143. Marshall, A.; Schulte to Bühne, H.; Bland, L.; Pettoelli, N. Assessing Ecosystem Collapse Risk in Ecosystems Dominated by Foundation Species: The Case of Fringe Mangroves. *Ecol. Indic.* **2018**, *91*, 128–137. [[CrossRef](#)]
144. Chen, Y.-C.; Chu, T.-J.; Wei, J.-D.; Shih, C.-H. Effects of Mangrove Removal on Benthic Organisms in the Siangshan Wetland in Hsinchu, Taiwan. *PeerJ.* **2018**, *6*, e5670. [[CrossRef](#)]
145. Staben, G.; Lucieer, A.; Scarth, P. Modelling LiDAR Derived Tree Canopy Height from Landsat TM, ETM+ and OLI Satellite Imagery—A Machine Learning Approach. *Int. J. Appl. Earth Obs. Geoinf.* **2018**, *73*, 666–681. [[CrossRef](#)]
146. Wan, R.; Wang, P.; Wang, X.; Yao, X.; Dai, X. Modeling Wetland Aboveground Biomass in the Poyang Lake National Nature Reserve Using Machine Learning Algorithms and Landsat-8 Imagery. *J. Appl. Remote Sens.* **2018**, *12*, 046029. [[CrossRef](#)]
147. Selvam, P.P.; Ramesh, R.; Purvaja, R.; Srinivasalu, S. Temporal Changes in Mangrove Forest Coverage and Seasonal Influence on NDVI in Pichavaram Mangrove Forest, India. *Int. J. Ecol. Dev.* **2019**, *34*, 49–61.
148. Taureau, F.; Robin, M.; Proisy, C.; Fromard, F.; Imbert, D.; Debaine, F. Mapping the Mangrove Forest Canopy Using Spectral Unmixing of Very High Spatial Resolution Satellite Images. *Remote Sens.* **2019**, *11*, 367. [[CrossRef](#)]

149. Shrestha, S.; Miranda, I.; Kumar, A.; Pardo, M.L.E.; Dahal, S.; Rashid, T.; Remillard, C.; Mishra, D.R. Identifying and Forecasting Potential Biophysical Risk Areas within a Tropical Mangrove Ecosystem Using Multi-Sensor Data. *Int. J. Appl. Earth Obs. Geoinf.* **2019**, *74*, 281–294. [[CrossRef](#)]
150. Roy, S.; Mahapatra, M.; Chakraborty, A. Mapping and Monitoring of Mangrove along the Odisha Coast Based on Remote Sensing and GIS Techniques. *Modeling Earth Syst. Environ.* **2019**, *5*, 217–226. [[CrossRef](#)]
151. Mafi-Gholami, D.; Zenner, E.K.; Jaafari, A.; Ward, R.D. Modeling Multi-Decadal Mangrove Leaf Area Index in Response to Drought along the Semi-Arid Southern Coasts of Iran. *Sci. Total Environ.* **2019**, *656*, 1326–1336. [[CrossRef](#)]
152. Bera, R.; Maiti, R. Quantitative Analysis of Erosion and Accretion (1975–2017) Using DSAS—A Study on Indian Sundarbans. *Reg. Stud. Mar. Sci.* **2019**, *28*, 100583. [[CrossRef](#)]
153. Alejandro Berlanga-Robles, C.; Ruiz-Luna, A.; Nepita Villanueva, M.R. Seasonal Trend Analysis (STA) of MODIS Vegetation Index Time Series for the Mangrove Canopy of the Teacapan-Agua Brava Lagoon System, Mexico. *GIScience Remote Sens.* **2019**, *56*, 338–361. [[CrossRef](#)]
154. Chuai, X.; Yuan, Y.; Zhang, X.; Guo, X.; Zhang, X.; Xie, F.; Zhao, R.; Li, J. Multiangle Land Use-Linked Carbon Balance Examination in Nanjing City, China. *Land Use Policy* **2019**, *84*, 305–315. [[CrossRef](#)]
155. Calva, L.G.; Golubov, J.; Mandujano, M.D.C.; Lara-Domínguez, A.L.; López-Portillo, J. Assessing Google Earth Pro Images for Detailed Conservation Diagnostics of Mangrove Communities. *Coas* **2019**, *92*, 33–43. [[CrossRef](#)]
156. Zhu, X.; Song, L.; Weng, Q.; Huang, G. Linking in Situ Photochemical Reflectance Index Measurements with Mangrove Carbon Dynamics in a Subtropical Coastal Wetland. *J. Geophys. Res. Biogeosci.* **2019**, *124*, 1714–1730. [[CrossRef](#)]
157. Yaney-Keller, A.; Tomillo, P.S.; Marshall, J.M.; Paladino, F.V. Using Unmanned Aerial Systems (UAS) to Assay Mangrove Estuaries on the Pacific Coast of Costa Rica. *PLoS ONE* **2019**, *14*, e0217310. [[CrossRef](#)]
158. Santos, R.D.O.; Delgado, R.C.; Pereira, M.G.; de Souza, L.P.; Tedoro, P.E.; da Silva Junior, C.A.; Costa, G.D.O. Space-Time Variability of the Roncador River Basin in the Change of Land Use and Cover and Its Correlation with Climatic Variables. *Biosci. J.* **2019**, *35*, 1033–1042. [[CrossRef](#)]
159. Vázquez-Lule, A.; Colditz, R.; Herrera-Silveira, J.; Guevara, M.; Rodríguez-Zúñiga, M.T.; Cruz, I.; Ressler, R.; Vargas, R. Greenness Trends and Carbon Stocks of Mangroves across Mexico. *Environ. Res. Lett.* **2019**, *14*, 075010. [[CrossRef](#)]
160. Pandey, P.C.; Anand, A.; Srivastava, P.K. Spatial Distribution of Mangrove Forest Species and Biomass Assessment Using Field Inventory and Earth Observation Hyperspectral Data. *Biodivers. Conserv.* **2019**, *28*, 2143–2162. [[CrossRef](#)]
161. Faridah-Hanum, I.; Yusoff, F.M.; Fitrianto, A.; Ainuddin, N.A.; Gandaseca, S.; Zaiton, S.; Norizah, K.; Nurhidayu, S.; Roslan, M.K.; Hakeem, K.R.; et al. Development of a Comprehensive Mangrove Quality Index (MQI) in Matang Mangrove: Assessing Mangrove Ecosystem Health. *Ecol. Indic.* **2019**, *102*, 103–117. [[CrossRef](#)]
162. Li, W.; El-Askary, H.; Qurban, M.A.; Li, J.; ManiKandan, K.P.; Piechota, T. Using Multi-Indices Approach to Quantify Mangrove Changes over the Western Arabian Gulf along Saudi Arabia Coast. *Ecol. Indic.* **2019**, *102*, 734–745. [[CrossRef](#)]
163. Zhang, C.; Durgan, S.D.; Lagomasino, D. Modeling Risk of Mangroves to Tropical Cyclones: A Case Study of Hurricane Irma. *Estuar. Coast. Shelf Sci.* **2019**, *224*, 108–116. [[CrossRef](#)]
164. Li, Q.; Wong, F.K.K.; Fung, T. Classification of Mangrove Species Using Combined WorldView-3 and LiDAR Data in Mai Po Nature Reserve, Hong Kong. *Remote Sens.* **2019**, *11*, 2114. [[CrossRef](#)]
165. Ashournejad, Q.; Amiraslani, F.; Moghadam, M.K.; Toomanian, A. Assessing the Changes of Mangrove Ecosystem Services Value in the Pars Special Economic Energy Zone. *Ocean Coast. Manag.* **2019**, *179*, 104838. [[CrossRef](#)]
166. Rayegani, B.; Barati, S.; Goshtasb, H.; Sarkheil, H.; Ramezani, J. An Effective Approach to Selecting the Appropriate Pan-Sharpener Method in Digital Change Detection of Natural Ecosystems. *Ecol. Inform.* **2019**, *53*, 100984. [[CrossRef](#)]
167. Li, H.; Jia, M.; Zhang, R.; Ren, Y.; Wen, X. Incorporating the Plant Phenological Trajectory into Mangrove Species Mapping with Dense Time Series Sentinel-2 Imagery and the Google Earth Engine Platform. *Remote Sens.* **2019**, *11*, 2479. [[CrossRef](#)]
168. Garcia del Toro, E.M.; Mas-Lopez, M.I. Changes in Land Cover in Cacheu River Mangroves Natural Park, Guinea-Bissau: The Need for a More Sustainable Management. *Sustainability* **2019**, *11*, 6247. [[CrossRef](#)]
169. Younes, N.; Joyce, K.E.; Northfield, T.D.; Maier, S.W. The Effects of Water Depth on Estimating Fractional Vegetation Cover in Mangrove Forests. *Int. J. Appl. Earth Obs. Geoinf.* **2019**, *83*, 101924. [[CrossRef](#)]
170. Rhyms, P.P.; Norizah, K.; Hamdan, O.; Faridah-Hanum, I.; Zulfa, A.W. Integration of Normalised Different Vegetation Index and Soil-Adjusted Vegetation Index for Mangrove Vegetation Delineation. *Remote Sens. Appl. Soc. Environ.* **2020**, *17*, 100280. [[CrossRef](#)]
171. Marins, R.V.; Lacerda, L.D.; Araujo, I.C.S.; Fonseca, L.V.; Silva, F.A. Phosphorus and Suspended Matter Retention in Mangroves Affected by Shrimp Farm Effluents in NE Brazil. *An. Acad. Bras. Ciênc.* **2020**, *92*, e20200758. [[CrossRef](#)]
172. Mandal, M.S.H.; Kamruzzaman, M.; Hosaka, T. Elucidating the Phenology of the Sundarbans Mangrove Forest Using 18-Year Time Series of MODIS Vegetation Indices. *Tropics* **2020**, *29*, 41–55. [[CrossRef](#)]
173. Xiao, H.; Su, F.; Fu, D.; Wang, Q.; Huang, C. Coastal Mangrove Response to Marine Erosion: Evaluating the Impacts of Spatial Distribution and Vegetation Growth in Bangkok Bay from 1987 to 2017. *Remote Sens.* **2020**, *12*, 220. [[CrossRef](#)]
174. Svejkovsky, J.; Ogurcak, D.E.; Ross, M.S.; Arkowitz, A. Satellite Image-Based Time Series Observations of Vegetation Response to Hurricane Irma in the Lower Florida Keys. *Estuaries Coasts* **2020**, *43*, 1058–1069. [[CrossRef](#)]
175. Chen, N. Mapping Mangrove in Dongzhaigang, China Using Sentinel-2 Imagery. *J. Appl. Remote Sens.* **2020**, *14*, 014508. [[CrossRef](#)]

176. Anand, A.; Pandey, P.C.; Petropoulos, G.P.; Pavlides, A.; Srivastava, P.K.; Sharma, J.K.; Malhi, R.K.M. Use of Hyperion for Mangrove Forest Carbon Stock Assessment in Bhitarkanika Forest Reserve: A Contribution towards Blue Carbon Initiative. *Remote Sens.* **2020**, *12*, 597. [[CrossRef](#)]
177. Arshad, M.; Eid, E.M.; Hasan, M. Mangrove Health along the Hyper-Arid Southern Red Sea Coast of Saudi Arabia. *Environ. Monit. Assess.* **2020**, *192*, 189. [[CrossRef](#)] [[PubMed](#)]
178. Thakur, S.; Maity, D.; Mondal, I.; Basumatary, G.; Ghosh, P.B.; Das, P.; De, T.K. Assessment of Changes in Land Use, Land Cover, and Land Surface Temperature in the Mangrove Forest of Sundarbans, Northeast Coast of India. *Environ. Dev. Sustain.* **2021**, *23*, 1917–1943. [[CrossRef](#)]
179. Bindu, G.; Rajan, P.; Jishnu, E.S.; Joseph, K.A. Carbon Stock Assessment of Mangroves Using Remote Sensing and Geographic Information System. *Egypt. J. Remote Sens. Space Sci.* **2020**, *23*, 1–9. [[CrossRef](#)]
180. Nguyen, H.-H.; Tran, L.T.N.; Le, A.T.; Nghia, N.H.; Duong, L.V.K.; Nguyen, H.T.T.; Bohm, S.; Premnath, C.F.S. Monitoring Changes in Coastal Mangrove Extents Using Multi-Temporal Satellite Data in Selected Communes, Hai Phong City, Vietnam. *For. Soc.* **2020**, *4*, 256–270. [[CrossRef](#)]
181. Mandal, M.S.H.; Hosaka, T. Assessing Cyclone Disturbances (1988–2016) in the Sundarbans Mangrove Forests Using Landsat and Google Earth Engine. *Nat. Hazards* **2020**, *102*, 133–150. [[CrossRef](#)]
182. Rossi, R.E.; Archer, S.K.; Giri, C.; Layman, C.A. The Role of Multiple Stressors in a Dwarf Red Mangrove (*Rhizophora Mangle*) Dieback. *Estuar. Coast. Shelf Sci.* **2020**, *237*, 106660. [[CrossRef](#)]
183. Le, H.T.; Tran, T.V.; Gyeltshen, S.; Nguyen, C.P.T.; Tran, D.X.; Luu, T.H.; Duong, M.B. Characterizing Spatiotemporal Patterns of Mangrove Forests in Can Gio Biosphere Reserve Using Sentinel-2 Imagery. *Appl. Sci.* **2020**, *10*, 4058. [[CrossRef](#)]
184. Taillie, P.J.; Roman-Cuesta, R.; Lagomasino, D.; Cifuentes-Jara, M.; Fatoyinbo, T.; Ott, L.E.; Poulter, B. Widespread Mangrove Damage Resulting from the 2017 Atlantic Mega Hurricane Season. *Environ. Res. Lett.* **2020**, *15*, 064010. [[CrossRef](#)]
185. Nur, H.; Islam, M.N. Hot Spot (Gi*) Model for Forest Vulnerability Assessment: A Remote Sensing-Based Geo-Statistical Investigation of the Sundarbans Mangrove Forest, Bangladesh. *Modeling Earth Syst. Environ.* **2020**, *6*, 2141–2151.
186. Sakti, A.D.; Fauzi, A.I.; Wilwatikta, F.N.; Rajagukguk, Y.S.; Sudhana, S.A.; Yayusman, L.F.; Syahid, L.N.; Sritarapipat, T.; Principe, J.A.; Trang, N.T.Q. Multi-Source Remote Sensing Data Product Analysis: Investigating Anthropogenic and Naturogenic Impacts on Mangroves in Southeast Asia. *Remote Sens.* **2020**, *12*, 2720. [[CrossRef](#)]
187. Dayathilake, D.D.T.L.; Lokupitiya, E.; Wijeratne, V.P.I.S. Estimation of Aboveground and Belowground Carbon Stocks in Urban Freshwater Wetlands of Sri Lanka. *Carbon Balance Manag.* **2020**, *15*, 17. [[CrossRef](#)] [[PubMed](#)]
188. Yu, M.; Gao, Q. Topography, Drainage Capability, and Legacy of Drought Differentiate Tropical Ecosystem Response to and Recovery from Major Hurricanes. *Environ. Res. Lett.* **2020**, *15*, 104046. [[CrossRef](#)]
189. Castillo, Y.B.; Kim, K.; Kim, H.S. Thirty-Two Years of Mangrove Forest Land Cover Change in Parita Bay, Panama. *For. Sci. Technol.* **2021**, *17*, 67–79. [[CrossRef](#)]
190. Etemadi, H.; Smoak, J.M.; Abbasi, E. Spatiotemporal Pattern of Degradation in Arid Mangrove Forests of the Northern Persian Gulf. *Oceanologia* **2021**, *63*, 99–114. [[CrossRef](#)]
191. Aljahdali, M.O.; Munawar, S.; Khan, W.R. Monitoring Mangrove Forest Degradation and Regeneration: Landsat Time Series Analysis of Moisture and Vegetation Indices at Rabigh Lagoon, Red Sea. *Forests* **2021**, *12*, 52. [[CrossRef](#)]
192. Nardin, W.; Vona, I.; Fagherazzi, S. Sediment Deposition Affects Mangrove Forests in the Mekong Delta, Vietnam. *Cont. Shelf Res.* **2021**, *213*, 104319. [[CrossRef](#)]
193. Valderrama-Landeros, L.; Flores-Verdugo, F.; Rodríguez-Sobreyra, R.; Kovacs, J.M.; Flores-de-Santiago, F. Extrapolating Canopy Phenology Information Using Sentinel-2 Data and the Google Earth Engine Platform to Identify the Optimal Dates for Remotely Sensed Image Acquisition of Semiarid Mangroves. *J. Environ. Manag.* **2021**, *279*, 111617. [[CrossRef](#)]
194. Thakur, S.; Mondal, I.; Bar, S.; Nandi, S.; Ghosh, P.B.; Das, P.; De, T.K. Shoreline Changes and Its Impact on the Mangrove Ecosystems of Some Islands of Indian Sundarbans, North-East Coast of India. *J. Clean. Prod.* **2021**, *284*, 124764. [[CrossRef](#)]
195. Zhao, C.-P.; Qin, C.-Z. A Detailed Mangrove Map of China for 2019 Derived from Sentinel-1 and -2 Images and Google Earth Images. *Geosci. Data J.* **2022**, *9*, 74–88. [[CrossRef](#)]
196. Jiang, Y.; Zhang, L.; Yan, M.; Qi, J.; Fu, T.; Fan, S.; Chen, B. High-Resolution Mangrove Forests Classification with Machine Learning Using Worldview and Uav Hyperspectral Data. *Remote Sens.* **2021**, *13*, 1529. [[CrossRef](#)]
197. Purnamasari, E.; Kamal, M.; Wicaksono, P. Comparison of Vegetation Indices for Estimating Above-Ground Mangrove Carbon Stocks Using PlanetScope Image. *Reg. Stud. Mar. Sci.* **2021**, *44*, 101730. [[CrossRef](#)]
198. Lee, C.K.; Duncan, C.; Nicholson, E.; Fatoyinbo, T.E.; Lagomasino, D.; Thomas, N.; Worthington, T.A.; Murray, N.J. Mapping the Extent of Mangrove Ecosystem Degradation by Integrating an Ecological Conceptual Model with Satellite Data. *Remote Sens.* **2021**, *13*, 2047. [[CrossRef](#)]
199. Cui, L.; Zuo, X.; Dou, Z.; Huang, Y.; Zhao, X.; Zhai, X.; Lei, Y.; Li, J.; Pan, X.; Li, W. Plant Identification of Beijing Hanshiqiao Wetland Based on Hyperspectral Data. *Spectrosc. Lett.* **2021**, *54*, 381–394. [[CrossRef](#)]
200. Obida, C.B.; Blackburn, G.A.; Whyatt, J.D.; Semple, K.T. Counting the Cost of the Niger Delta's Largest Oil Spills: Satellite Remote Sensing Reveals Extensive Environmental Damage with >1million People in the Impact Zone. *Sci. Total Environ.* **2021**, *775*, 145854. [[CrossRef](#)]
201. Niu, C.; Phinn, S.; Roelfsema, C. Global Sensitivity Analysis for Canopy Reflectance and Vegetation Indices of Mangroves. *Remote Sens.* **2021**, *13*, 2617. [[CrossRef](#)]

202. Singgalen, Y.A.; Gudiato, C.; Prasetyo, S.Y.J.; Fibriani, C. Mangrove Monitoring Using Normalized Difference Vegetation Index (NDVI): Case Study In North Halmahera, Indonesia. *J. Teknol. Kelaut. Trop.* **2021**, *13*, 219–239. [[CrossRef](#)]
203. Kamal, M.; Sidik, F.; Prananda, A.R.A.; Mahardhika, S.A. Mapping Leaf Area Index of Restored Mangroves Using WorldView-2 Imagery in Perancak Estuary, Bali, Indonesia. *Remote Sens. Appl. Soc. Environ.* **2021**, *23*, 100567. [[CrossRef](#)]
204. Maina, J.M.; Bosire, J.O.; Kairo, J.G.; Bandeira, S.O.; Mangora, M.M.; Macamo, C.; Ralison, H.; Majambo, G. Identifying Global and Local Drivers of Change in Mangrove Cover and the Implications for Management. *Glob. Ecol. Biogeogr.* **2021**, *30*, 2057–2069. [[CrossRef](#)]
205. Idris, N.S.; Mustapha, M.A.; Sulaiman, N.; Khamis, S.; Husin, S.M.; Darbis, N.D.A. The Dynamics of Landscape Changes Surrounding a Firefly Ecotourism Area. *Glob. Ecol. Conserv.* **2021**, *29*, e01741. [[CrossRef](#)]
206. Mishra, M.; Acharyya, T.; Santos, C.A.G.; da Silva, R.M.; Kar, D.; Mustafa Kamal, A.H.; Raulo, S. Geo-Ecological Impact Assessment of Severe Cyclonic Storm Amphan on Sundarban Mangrove Forest Using Geospatial Technology. *Estuar. Coast. Shelf Sci.* **2021**, *260*, 107486. [[CrossRef](#)]
207. Nguyen, H.-H.; Nguyen, T.T.H. Above-Ground Biomass Estimation Models of Mangrove Forests Based on Remote Sensing and Field-Surveyed Data: Implications for C-PFES Implementation in Quang Ninh Province, Vietnam. *Reg. Stud. Mar. Sci.* **2021**, *48*, 101985. [[CrossRef](#)]
208. Meijer, K.J.; El-Hacen, E.-H.M.; Govers, L.L.; Lavaleye, M.; Piersma, T.; Olf, H. Mangrove-Mudflat Connectivity Shapes Benthic Communities in a Tropical Intertidal System. *Ecol. Indic.* **2021**, *130*, 108030. [[CrossRef](#)]
209. Guo, X.; Wang, M.; Jia, M.; Wang, W. Estimating Mangrove Leaf Area Index Based on Red-Edge Vegetation Indices: A Comparison among UAV, WorldView-2 and Sentinel-2 Imagery. *Int. J. Appl. Earth Obs. Geoinf.* **2021**, *103*, 102493. [[CrossRef](#)]
210. Barr, J.G.; Engel, V.; Smith, T.J.; Fuentes, J.D. Hurricane Disturbance and Recovery of Energy Balance, CO₂ Fluxes and Canopy Structure in a Mangrove Forest of the Florida Everglades. *Agric. For. Meteorol.* **2012**, *153*, 54–66. [[CrossRef](#)]
211. Barr, J.G.; Engel, V.; Fuentes, J.D.; Fuller, D.O.; Kwon, H. Modeling Light Use Efficiency in a Subtropical Mangrove Forest Equipped with CO₂ Eddy Covariance. *Biogeosciences* **2013**, *10*, 2145–2158. [[CrossRef](#)]
212. Shoemaker, W.B.; Anderson, F.; Barr, J.G.; Graham, S.L.; Botkin, D.B. Carbon Exchange between the Atmosphere and Subtropical Forested Cypress and Pine Wetlands. *Biogeosciences* **2015**, *12*, 2285–2300. [[CrossRef](#)]
213. Dutta, D.; Das, P.K.; Paul, S.; Sharma, J.R.; Dadhwal, V.K. Assessment of Ecological Disturbance in the Mangrove Forest of Sundarbans Caused by Cyclones Using MODIS Time-Series Data (2001–2011). *Nat. Hazards* **2015**, *79*, 775–790. [[CrossRef](#)]
214. Ishtiaque, A.; Myint, S.W.; Wang, C. Examining the Ecosystem Health and Sustainability of the World's Largest Mangrove Forest Using Multi-Temporal MODIS Products. *Sci. Total Environ.* **2016**, *569–570*, 1241–1254. [[CrossRef](#)]
215. Bolivar, J.M.; Gutierrez-Velez, V.H.; Sierra, C.A. Carbon Stocks in Aboveground Biomass for Colombian Mangroves with Associated Uncertainties. *Reg. Stud. Mar. Sci.* **2018**, *18*, 145–155. [[CrossRef](#)]
216. Songsom, V.; Koedsin, W.; Ritchie, R.J.; Huete, A. Mangrove Phenology and Environmental Drivers Derived from Remote Sensing in Southern Thailand. *Remote Sens.* **2019**, *11*, 955. [[CrossRef](#)]
217. Nepita-Villanueva, M.R.; Berlanga-Robles, C.A.; Ruiz-Luna, A.; Morales Barcenas, J.H. Spatio-Temporal Mangrove Canopy Variation (2001–2016) Assessed Using the MODIS Enhanced Vegetation Index (EVI). *J. Coast. Conserv.* **2019**, *23*, 589–597. [[CrossRef](#)]
218. Feagin, R.A.; Forbrich, I.; Huff, T.P.; Barr, J.G.; Ruiz-Plancarte, J.; Fuentes, J.D.; Najjar, R.G.; Vargas, R.; Vázquez-Lule, A.; Windham-Myers, L. Tidal Wetland Gross Primary Production across the Continental United States, 2000–2019. *Glob. Biogeochem. Cycles* **2020**, *34*, e2019GB006349. [[CrossRef](#)]
219. Berlanga-Robles, C.A.; Ruiz-Luna, A. Assessing Seasonal and Long-Term Mangrove Canopy Variations in Sinaloa, Northwest Mexico, Based on Time Series of Enhanced Vegetation Index (EVI) Data. *Wetl. Ecol. Manag.* **2020**, *28*, 229–249. [[CrossRef](#)]
220. Parida, B.R.; Kumari, A. Mapping and Modeling Mangrove Biophysical and Biochemical Parameters Using Sentinel-2A Satellite Data in Bhitarkanika National Park, Odisha. *Model. Earth Syst. Environ.* **2021**, *7*, 2463–2474. [[CrossRef](#)]
221. Younes, N.; Northfield, T.D.; Joyce, K.E.; Maier, S.W.; Duke, N.C.; Lymburner, L. A Novel Approach to Modelling Mangrove Phenology from Satellite Images: A Case Study from Northern Australia. *Remote Sens.* **2020**, *12*, 4008. [[CrossRef](#)]
222. Younes, N.; Joyce, K.E.; Maier, S.W. All Models of Satellite-Derived Phenology Are Wrong, but Some Are Useful: A Case Study from Northern Australia. *Int. J. Appl. Earth Obs. Geoinf.* **2021**, *97*, 102285. [[CrossRef](#)]
223. Peereman, J.; Hogan, J.A.; Lin, T.-C. Disturbance Frequency, Intensity and Forest Structure Modulate Cyclone-Induced Changes in Mangrove Forest Canopy Cover. *Glob. Ecol. Biogeogr.* **2022**, *31*, 37–50. [[CrossRef](#)]
224. Zhu, B.; Liao, J.; Shen, G. Spatio-Temporal Simulation of Mangrove Forests under Different Scenarios: A Case Study of Mangrove Protected Areas, Hainan Island, China. *Remote Sens.* **2021**, *13*, 4059. [[CrossRef](#)]
225. Poortinga, A.; Tenneson, K.; Shapiro, A.; Nguyen, Q.; San Aung, K.; Chishtie, F.; Saah, D. Mapping Plantations in Myanmar by Fusing Landsat-8, Sentinel-2 and Sentinel-1 Data along with Systematic Error Quantification. *Remote Sens.* **2019**, *11*, 831. [[CrossRef](#)]
226. Tucker, C.J. Red and Photographic Infrared Linear Combinations for Monitoring Vegetation. *Remote Sens. Environ.* **1979**, *8*, 127–150. [[CrossRef](#)]
227. Liu, X.; Wang, L. Feasibility of Using Consumer-Grade Unmanned Aerial Vehicles to Estimate Leaf Area Index in Mangrove Forest. *Remote Sens. Lett.* **2018**, *9*, 1040–1049. [[CrossRef](#)]

228. Clevers, J. The Application of a Vegetation Index in Correcting the Infrared Reflectance for Soil Background. In Proceedings of the Remote Sensing for Resources Development and Environmental Management, International Symposium. 7, Enschede, The Netherlands, 25–29 August 1986; pp. 221–226.
229. Major, D.J.; Baret, F.; Guyot, G. A Ratio Vegetation Index Adjusted for Soil Brightness. *Int. J. Remote Sens.* **1990**, *11*, 727–740. [[CrossRef](#)]
230. Pinty, B.; Verstraete, M.M. GEMI: A Non-Linear Index to Monitor Global Vegetation from Satellites. *Vegetatio* **1992**, *101*, 15–20. [[CrossRef](#)]
231. Kaufman, Y.J.; Tanre, D. Atmospherically Resistant Vegetation Index (ARVI) for EOS-MODIS. *IEEE Trans. Geosci. Remote Sens.* **1992**, *30*, 261–270. [[CrossRef](#)]
232. Hati, J.P.; Goswami, S.; Samanta, S.; Pramanick, N.; Majumdar, S.D.; Chaube, N.R.; Misra, A.; Hazra, S. Estimation of Vegetation Stress in the Mangrove Forest Using AVIRIS-NG Airborne Hyperspectral Data. *Modeling Earth Syst. Environ.* **2021**, *7*, 1877–1889. [[CrossRef](#)]
233. Goel, N.S.; Qin, W. Influences of Canopy Architecture on Relationships between Various Vegetation Indices and LAI and Fpar: A Computer Simulation. *Remote Sens. Rev.* **1994**, *10*, 309–347. [[CrossRef](#)]
234. Qi, J.; Chehbouni, A.; Huete, A.R.; Kerr, Y.H.; Sorooshian, S. A Modified Soil Adjusted Vegetation Index. *Remote Sens. Environ.* **1994**, *48*, 119–126. [[CrossRef](#)]
235. Roujean, J.-L.; Breon, F.-M. Estimating PAR Absorbed by Vegetation from Bidirectional Reflectance Measurements. *Remote Sens. Environ.* **1995**, *51*, 375–384. [[CrossRef](#)]
236. Chen, J.M. Evaluation of Vegetation Indices and a Modified Simple Ratio for Boreal Applications. *Can. J. Remote Sens.* **1996**, *22*, 229–242. [[CrossRef](#)]
237. Gitelson, A.A.; Kaufman, Y.J.; Merzlyak, M.N. Use of a Green Channel in Remote Sensing of Global Vegetation from EOS-MODIS. *Remote Sens. Environ.* **1996**, *58*, 289–298. [[CrossRef](#)]
238. Rondeaux, G.; Steven, M.; Baret, F. Optimization of Soil-Adjusted Vegetation Indices. *Remote Sens. Environ.* **1996**, *55*, 95–107. [[CrossRef](#)]
239. Gitelson, A.A.; Merzlyak, M.N. Remote Sensing of Chlorophyll Concentration in Higher Plant Leaves. *Adv. Space Res.* **1998**, *22*, 689–692. [[CrossRef](#)]
240. Louhaichi, M.; Borman, M.M.; Johnson, D.E. Spatially Located Platform and Aerial Photography for Documentation of Grazing Impacts on Wheat. *Geocarto Int.* **2001**, *16*, 65–70. [[CrossRef](#)]
241. Broge, N.H.; Leblanc, E. Comparing Prediction Power and Stability of Broadband and Hyperspectral Vegetation Indices for Estimation of Green Leaf Area Index and Canopy Chlorophyll Density. *Remote Sens. Environ.* **2001**, *76*, 156–172. [[CrossRef](#)]
242. Bannari, A.; Asalhi, H.; Teillet, P.M. Transformed Difference Vegetation Index (TDVI) for Vegetation Cover Mapping. In Proceedings of the IEEE International geoscience and remote sensing symposium, Toronto, ON, Canada, 24–28 June 2002; Volume 5, pp. 3053–3055.
243. Gong, P.; Pu, R.; Biging, G.S.; Larrieu, M.R. Estimation of Forest Leaf Area Index Using Vegetation Indices Derived from Hyperion Hyperspectral Data. *IEEE Trans. Geosci. Remote Sens.* **2003**, *41*, 1355–1362. [[CrossRef](#)]
244. Haboudane, D.; Miller, J.R.; Pattey, E.; Zarco-Tejada, P.J.; Strachan, I.B. Hyperspectral Vegetation Indices and Novel Algorithms for Predicting Green LAI of Crop Canopies: Modeling and Validation in the Context of Precision Agriculture. *Remote Sens. Environ.* **2004**, *90*, 337–352. [[CrossRef](#)]
245. Vincini, M.; Frazzi, E.; D’Alessio, P.; Stafford, J.V. Comparison of Narrow-Band and Broad-Band Vegetation Indexes for Canopy Chlorophyll Density Estimation in Sugar Beet. In Proceedings of the Precision agriculture ‘07: Proceedings of the 6th European Conference on Precision Agriculture, Skiathos, Greece, 3–6 June 2007; pp. 189–196.
246. Rahman, A.F.; Dragoni, D.; Didan, K.; Barreto-Munoz, A.; Hutabarat, J.A. Detecting Large Scale Conversion of Mangroves to Aquaculture with Change Point and Mixed-Pixel Analyses of High-Fidelity MODIS Data. *Remote Sens. Environ.* **2013**, *130*, 96–107. [[CrossRef](#)]
247. Muhsoni, F.F.; Sambah, A.B.; Mahmudi, M.; Wiadnya, D.G.R. Comparison of Different Vegetation Indices for Assessing Mangrove Density Using Sentinel-2 Imagery. *GEOMATE J.* **2018**, *14*, 42–51.
248. Woebbecke, D.; Meyer, G.; Barga, K.V.; Mortensen, D. Color Indices for Weed Identification under Various Soil, Residue, and Lighting Conditions. *Trans. ASAE* **1995**, *38*, 259–269. [[CrossRef](#)]
249. Gitelson, A.; Merzlyak, M.N. Spectral Reflectance Changes Associated with Autumn Senescence of *Aesculus Hippocastanum* L. and *Acer Platanoides* L. Leaves. Spectral Features and Relation to Chlorophyll Estimation. *J. Plant Physiol.* **1994**, *143*, 286–292. [[CrossRef](#)]
250. Merzlyak, M.N.; Gitelson, A.A.; Chivkunova, O.B.; Rakitin, V.Y. Non-destructive Optical Detection of Pigment Changes during Leaf Senescence and Fruit Ripening. *Physiol. Plant.* **1999**, *106*, 135–141. [[CrossRef](#)]
251. Barnes, E.M.; Clarke, T.R.; Richards, S.E.; Colaizzi, P.D.; Haberland, J.; Kostrzewski, M.; Waller, P.; Choi, C.; Riley, E.; Thompson, T. Coincident Detection of Crop Water Stress, Nitrogen Status and Canopy Density Using Ground Based Multispectral Data. In Proceedings of the Fifth International Conference on Precision Agriculture, Bloomington, MN, USA, 16–19 July 2000; Volume 1619.
252. Gitelson, A.A.; Viña, A.; Arkebauer, T.J.; Rundquist, D.C.; Keydan, G.; Leavitt, B. Remote Estimation of Leaf Area Index and Green Leaf Biomass in Maize Canopies. *Geophys. Res. Lett.* **2003**, *30*, 1248. [[CrossRef](#)]
253. Dash, J.; Curran, P.J. The MERIS Terrestrial Chlorophyll Index. *Int. J. Remote Sens.* **2004**, *25*, 5403–5413. [[CrossRef](#)]

254. Biswas, H.; Zhang, K.; Ross, M.S.; Gann, D. Delineation of Tree Patches in a Mangrove-Marsh Transition Zone by Watershed Segmentation of Aerial Photographs. *Remote Sens.* **2020**, *12*, 2086. [[CrossRef](#)]
255. Meyer, G.E.; Hindman, T.W.; Laksmi, K. *Machine Vision Detection Parameters for Plant Species Identification*; Meyer, G.E., DeShazer, J.A., Eds.; SPIE: Boston, MA, USA, 1999; pp. 327–335.
256. Gitelson, A.A.; Kaufman, Y.J.; Stark, R.; Rundquist, D. Novel Algorithms for Remote Estimation of Vegetation Fraction. *Remote Sens. Environ.* **2002**, *80*, 76–87. [[CrossRef](#)]
257. Kataoka, T.; Kaneko, T.; Okamoto, H.; Hata, S. Crop Growth Estimation System Using Machine Vision. In Proceedings of the Proceedings 2003 IEEE/ASME International Conference on Advanced Intelligent Mechatronics (AIM 2003), Kobe, Japan, 20–24 July 2003; Volume 2, pp. b1079–b1083.
258. Hague, T.; Tillett, N.D.; Wheeler, H. Automated Crop and Weed Monitoring in Widely Spaced Cereals. *Precis. Agric.* **2006**, *7*, 21–32. [[CrossRef](#)]
259. Meyer, G.E.; Neto, J.C. Verification of Color Vegetation Indices for Automated Crop Imaging Applications. *Comput. Electron. Agric.* **2008**, *63*, 282–293. [[CrossRef](#)]
260. Hunt, E.R.; Daughtry, C.S.T.; Eitel, J.U.; Long, D.S. Remote Sensing Leaf Chlorophyll Content Using a Visible Band Index. *Agron. J.* **2011**, *103*, 1090–1099. [[CrossRef](#)]
261. Yang, W.; Wang, S.; Zhao, X.; Zhang, J.; Feng, J. Greenness Identification Based on HSV Decision Tree. *Inf. Processing Agric.* **2015**, *2*, 149–160. [[CrossRef](#)]
262. Xiaoqin, W.; Miaomiao, W.; Shaoqiang, W.; Yundong, W. Extraction of Vegetation Information from Visible Unmanned Aerial Vehicle Images. *Trans. Chin. Soc. Agric. Eng.* **2015**, *31*, 152–159.
263. Spencer, T.; Möller, I.; Reef, R. Mangrove Systems and Environments. *Ref. Modul. Earth Syst. Environ. Sci.* **2022**, 675–712. [[CrossRef](#)]
264. Gao, B.-C. NDWI—A Normalized Difference Water Index for Remote Sensing of Vegetation Liquid Water from Space. *Remote Sens. Environ.* **1996**, *58*, 257–266. [[CrossRef](#)]
265. Bhatti, S.S.; Tripathi, N.K. Built-up Area Extraction Using Landsat 8 OLI Imagery. *GIScience Remote Sens.* **2014**, *51*, 445–467. [[CrossRef](#)]
266. Neri, M.P.; Baloloy, A.B.; Blanco, A.C. Limitation Assessment and Workflow Refinement of the Mangrove Vegetation Index (MVI)-Based Mapping Methodology Using Sentinel-2 Imagery. *Int. Arch. Photogramm. Remote Sens. Spat. Inf. Sci.* **2021**, *46*, 235–242. [[CrossRef](#)]
267. Kamal, M.; Phinn, S. Hyperspectral Data for Mangrove Species Mapping: A Comparison of Pixel-Based and Object-Based Approach. *Remote Sens.* **2011**, *3*, 2222–2242. [[CrossRef](#)]
268. Toosi, N.B.; Soffianian, A.R.; Fakheran, S.; Pourmanafi, S.; Ginzler, C.; Waser, L.T. Comparing Different Classification Algorithms for Monitoring Mangrove Cover Changes in Southern Iran. *Glob. Ecol. Conserv.* **2019**, *19*, e00662. [[CrossRef](#)]
269. Akhrianti, I. Spatial Distribution of Mangrove in Kelapan Island, South Bangka Regency. *Red* **2019**, *665*, 10.
270. Hardisky, M.A.; Daiber, F.C.; Roman, C.T.; Klemas, V. Remote Sensing of Biomass and Annual Net Aerial Primary Productivity of a Salt Marsh. *Remote Sens. Environ.* **1984**, *16*, 91–106. [[CrossRef](#)]
271. Xiao, X.; Zhang, Q.; Braswell, B.; Urbanski, S.; Boles, S.; Wofsy, S.; Moore, B.; Ojima, D. Modeling Gross Primary Production of Temperate Deciduous Broadleaf Forest Using Satellite Images and Climate Data. *Remote Sens. Environ.* **2004**, *91*, 256–270. [[CrossRef](#)]
272. Xu, H. Modification of Normalised Difference Water Index (NDWI) to Enhance Open Water Features in Remotely Sensed Imagery. *Int. J. Remote Sens.* **2006**, *27*, 3025–3033. [[CrossRef](#)]
273. Hirata, Y.; Tabuchi, R.; Patanaponpaiboon, P.; Pongparn, S.; Yoneda, R.; Fujioka, Y. Estimation of Aboveground Biomass in Mangrove Forests Using High-Resolution Satellite Data. *J. Res.* **2014**, *19*, 34–41. [[CrossRef](#)]
274. Bathmann, J.; Peters, R.; Reef, R.; Berger, U.; Walther, M.; Lovelock, C.E. Modelling Mangrove Forest Structure and Species Composition over Tidal Inundation Gradients: The Feedback between Plant Water Use and Porewater Salinity in an Arid Mangrove Ecosystem. *Agric. For. Meteorol.* **2021**, *308–309*, 108547. [[CrossRef](#)]
275. Fang, H.; Liang, S. Leaf Area Index Models. In *Reference Module in Earth Systems and Environmental Sciences*; Elsevier: Amsterdam, The Netherlands, 2014; pp. 2139–2148. ISBN 978-0-12-409548-9.
276. Zhen, J.; Jiang, X.; Xu, Y.; Miao, J.; Zhao, D.; Wang, J.; Wang, J.; Wu, G. Mapping Leaf Chlorophyll Content of Mangrove Forests with Sentinel-2 Images of Four Periods. *Int. J. Appl. Earth Obs. Geoinf.* **2021**, *102*, 102387. [[CrossRef](#)]
277. Hansen, M.C.; Potapov, P.V.; Moore, R.; Hancher, M.; Turubanova, S.A.; Tyukavina, A.; Thau, D.; Stehman, S.V.; Goetz, S.J.; Loveland, T.R.; et al. High-Resolution Global Maps of 21st-Century Forest Cover Change. *Science* **2013**, *342*, 850–853. [[CrossRef](#)] [[PubMed](#)]
278. Lehmann, E.A.; Wallace, J.F.; Caccetta, P.A.; Furby, S.L.; Zdunic, K. Forest Cover Trends from Time Series Landsat Data for the Australian Continent. *Int. J. Appl. Earth Obs. Geoinf.* **2013**, *21*, 453–462. [[CrossRef](#)]
279. Reddy, D.S.; Prasad, P.R.C. Prediction of Vegetation Dynamics Using NDVI Time Series Data and LSTM. *Modeling Earth Syst. Environ.* **2018**, *4*, 409–419. [[CrossRef](#)]
280. Bryan-Brown, D.N.; Connolly, R.M.; Richards, D.R.; Adame, F.; Friess, D.A.; Brown, C.J. Global Trends in Mangrove Forest Fragmentation. *Sci Rep.* **2020**, *10*, 7117. [[CrossRef](#)]

281. Kanniah, K.D.; Kang, C.S.; Sharma, S.; Amir, A.A. Remote Sensing to Study Mangrove Fragmentation and Its Impacts on Leaf Area Index and Gross Primary Productivity in the South of Peninsular Malaysia. *Remote Sens.* **2021**, *13*, 1427. [CrossRef]
282. USGS. USGS EROS Archive—Advanced Very High Resolution Radiometer (AVHRR)—Sensor Characteristics. Available online: <https://www.usgs.gov/centers/eros/science/usgs-eros-archive-advanced-very-high-resolution-radiometer-avhrr#web-tools> (accessed on 25 April 2022).